Journal Pre-proof



Electrical discharge-mechanical hybrid drilling of micro-holes in carbon fibre-reinforced polymers

Yijin Zhao, Xiaodong Yang, Yong Lu, Xiaoming Duan

PII: S0890-6955(24)00129-9

DOI: https://doi.org/10.1016/j.ijmachtools.2024.104243

Reference: MTM 104243

To appear in: *International Journal of Machine Tools and Manufacture*

Received Date: 2 July 2024

Revised Date: 14 December 2024

Accepted Date: 17 December 2024

Please cite this article as: Y. Zhao, X. Yang, Y. Lu, X. Duan, Electrical discharge-mechanical hybrid drilling of micro-holes in carbon fibre-reinforced polymers, *International Journal of Machine Tools and Manufacture*, https://doi.org/10.1016/j.ijmachtools.2024.104243.

Title: Electrical discharge-mechanical hybrid drilling of micro-holes in carbon fibre-reinforced polymers

Yijin Zhao[1], Xiaodong Yang[1], Yong Lu[1], Xiaoming Duan[*1]

[1]Department of Mechanical Engineering and Automation, Harbin Institute of Technology, Harbin, 150001, China

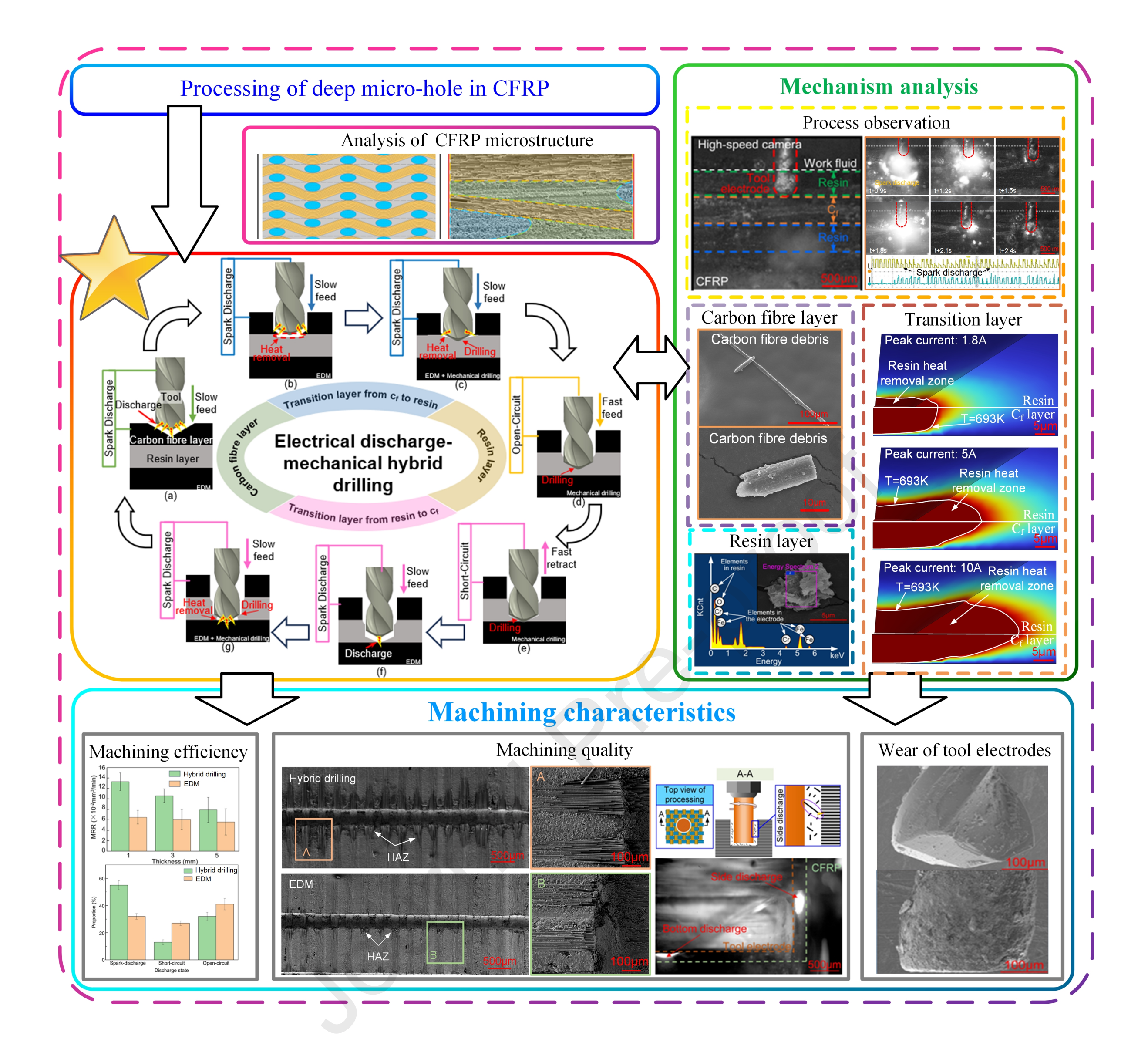
*Corresponding author
Name：Xiaoming Duan
Dept. of Mechanical Engineering and Automation
Harbin Institute of Technology
Add：Zhizao building, Room 516
P.O.421. Harbin Institute of Technology (150001)
Email: XiaomingDuan@hit.edu.cn
Tel.: 86-0451-86403845

Acknowledgement

This work was supported by the National Natural Science Foundation of China (General Program, No. 52375419); and the Postdoctoral Fellowship Program of CPSF (General Program, No. GZC20233455) for providing financial support for this research. The authors gratefully thank Prof. Dragos Axinte and Prof. Zhirong Liao of the University of Nottingham for their suggestions on the experimental plan for this paper.

Declaration of interests

The authors declare that they have no known competing financial interests or personal relationships that could have appeared to influence the work reported in this paper.



Processing of deep micro-hole in CFRP
Analysis of CFRP microstructure
Electrical discharge-mechanical hybrid drilling
Carbon fibre layer
Transition layer from C_f to resin
Resin layer
Transition layer from resin to C_f
Spark Discharge
Open-Circuit
Short-Circuit
Slow feed
Fast feed
Fast retract
Heat removal
Drilling
Discharge
Resin layer
Mechanism analysis
Process observation
High-speed camera
Work fluid
Tool electrode
Resin
CFRP
Spark discharge
Carbon fibre layer
Carbon fibre debris
Transition layer
Peak current: 1.8A
Peak current: 5A
Peak current: 10A
Resin heat removal zone
T=693K
C_f layer
Resin layer
Machining characteristics
Machining efficiency
Hybrid drilling
EDM
Thickness (mm)
Machining quality
HAZ
Top view of processing
A-A
Side discharge
Bottom discharge
Tool electrode
Wear of tool electrodes

1 Electrical discharge-mechanical hybrid drilling of micro-holes in carbon
2 fibre-reinforced polymers

3 **Abstract**:

4 The machining of deep micro-holes in carbon fibre-reinforced polymers (CFRP)
5 components exhibits a significantly increased demand in the industry. However, it is
6 difficult to machine CFRP deep micro-holes using conventional mechanical drilling
7 and non-conventional processes individually because of the anisotropic and
8 inhomogeneous characteristics of CFRP. To address this problem, an electrical
9 discharge-mechanical hybrid drilling method was proposed in this study. In this method,
10 a specialized servo control strategy was employed to effectively utilize the electrical
11 discharge machining and mechanical drilling, based on the distinct difference in
12 electrical conductivity between the carbon fibre and the resin in CFRP. This effectively
13 resolved the challenges posed by the high hardness of the carbon fibre for mechanical
14 drilling and the non-conductivity of the resin for EDM, taking advantage of both EDM
15 and mechanical drilling. High-speed photography, processing debris analysis, discharge
16 state monitoring, and finite element simulation were performed to investigate the
17 machining process and material removal mechanism of electrical discharge-mechanical
18 hybrid drilling. The results showed that most of the carbon fibre and resin were
19 individually removed by EDM and mechanical drilling, respectively. However, in the
20 interfacial region between the carbon fibre and resin, both mechanical drilling and EDM
21 occur simultaneously. The heat generated during the EDM of carbon fibre also leads to
22 the thermal decomposition and vaporization of the resin in proximity to the carbon fibre.
23 Furthermore, deep micro-holes machining with a diameter of 330μm and a depth-to-
24 diameter ratio of 15.1 was performed on CFRP component to validate the advantages
25 of the proposed hybrid drilling method. Compared with EDM, the proposed hybrid
26 machining method exhibited a 29.1% increase in efficiency, 56.25% reduction in taper,
27 and 54.32% reduction in the heat-affected zone. These outcomes demonstrate that the
28 electrical discharge-mechanical hybrid drilling holds great potential for machining
29 high-quality micro-holes on advanced multilayer composites with anisotropic and

30 inhomogeneous properties.

31 **Keywords:** Electrical discharge machining (EDM), Mechanical drilling, Hybrid
32 drilling, carbon fibre-reinforced polymers (CFRP), Micro-hole

33 1. Introduction

34 Carbon fibre-reinforced polymers (CFRP) have been widely used in the aerospace,
35 civil engineering, automotive, and sports industries [1,2], attributed to their high strength,
36 stiffness-to-weight ratio, corrosion resistance, and fatigue resistance [3]. Currently, the
37 machining of holes of different scales in CFRP is necessary for functions such as joining,
38 sensor implantation, and gas flow, enabling the CFRP material to become an end-use
39 component [4,5]. However, this material is non-homogeneous and anisotropic because of
40 the significant disparities in material properties between the two phases and the varying
41 properties of carbon fibre in different directions [6]. This causes great difficulties in the
42 high-quality machining of CFRP holes, especially in micro-hole machining.

43 There are two main methods for machining holes in CFRP: conventional
44 mechanical drilling and non-conventional processes such as abrasive water jet
45 machining (AWJM), laser machining, and electrical discharge machining (EDM).
46 Mechanical drilling is currently the mainstream method for hole machining of CFRP.
47 Jia et al. [7] proposed a novel drill structure designed to optimize the cutting conditions
48 at the drill exit, thereby effectively mitigating damage during mechanical drilling of
49 CFRP. Wang et al. [8] reported that edge rounding wear was the predominant wear
50 mechanism during CFRP drilling, and that diamond-coated drills exhibited
51 significantly lower wear compared to uncoated drills. However, the high hardness of
52 the carbon fibre in CFRP materials, combined with the weak bonding strength between
53 the fibre and the resin, leads to significant tool wear and causes machining-induced
54 damage such as delamination, burrs, and pull-out fibre [9]. In addition, when drilling
55 deep micro-holes in CFRP components, the high cutting forces during machining tend
56 to cause the drill bit fracture due to its low stiffness, rendering the machining impossible
57 [10]. Based on the statistical analysis of published papers to date, the depth-to-diameter
58 ratio of mechanically drilled CFRP holes is typically less than 3 (Fig. 1).

59 Compared to conventional mechanical drilling, non-conventional machining
60 processes such as AWJM [11] and laser machining [12] offer unique advantages, including
61 high manufacturing efficiency, reduced cutting forces, and improved cost-effectiveness
62 in the machining of CFRP holes. However, these methods still have inherent machining
63 challenges. For example, the high-pressure jet in the AWJM process promotes the
64 penetration of water molecules and abrasives into CFRP, degrading its mechanical
65 properties [13]. Delamination defects also tend to occur frequently during AWJM due to
66 the inhomogeneous properties of CFRP [14]. In addition, AWJM is unable to meet the
67 micro-hole machining requirements owing to the limitations of water jets and abrasive
68 sizes. The diameter of CFRP micro-holes processed by AWJM is challenging to reduce
69 below 1 mm (Fig. 1). Laser machining demonstrates superior capability in machining
70 CFRP micro-holes compared to AWJM. However, the machined holes using laser
71 exhibit a large heat-affected zone (HAZ) and taper owing to the difference in laser
72 absorption and reflectivity between the carbon fibre and resin, thus limiting the
73 machining of deep micro-holes [15,16]. Currently, the depth-to-diameter ratio of laser-
74 machined CFRP micro-hole is difficult to reach 10 (Fig. 1).

75 EDM is another non-traditional machining method, which removes material based
76 on the principle of electrical erosion by pulsed spark discharges between the tool
77 electrode and workpiece in a medium [17]. It can machine any electrically conductive
78 material and is especially suitable for machining special materials with high hardness,
79 strength, melting point, toughness, and brittleness [18]. Therefore, EDM exhibits
80 significant potential for high-quality micro-hole processing of CFRP [19] and has
81 attracted considerable academic interest. Habib et al. [20] claimed that the graphite
82 electrode exhibits relatively higher material removal rate than copper electrode during
83 EDM of CFRP hole. The electrode wear rate decreases with increasing pulse-off time
84 for both copper and graphite electrodes. Sheikh-Ahmad et al. [21] pointed out that pulse
85 on-time is the key parameter affecting the HAZ. Nevertheless, the aforementioned
86 studies are limited to revealing the effect of process parameters on the machining
87 quality and efficiency. There is a significant knowledge gap in understanding the

88 removal mechanism of the non-conductive resin layer during EDM of CFRP deep
89 micro-holes and how to address the limitations of the resin layer on the ability to EDM
90 deep micro-holes.

91 Statistics from related published articles show that EDM is difficult to achieve high
92 quality and efficient machining of deep micro-hole in CFRP (Fig. 1). Although Kumar
93 et al. [22] demonstrated that through-holes with a diameter of 110 μm and a depth of 1.2
94 mm can be successfully machined in CFRP using EDM, their study was limited to
95 machining within the carbon fibre layer, which differs from the more complex, multi-
96 layered nature of actual CFRP machining. The presence of a non-conductive resin layer
97 may induce unstable discharge conditions and increased tool electrode wear, limiting
98 the use of EDM for the high-quality machining of CFRP deep micro-holes. Therefore,
99 hybrid EDM and mechanical drilling have strong potential to address the challenges
100 arising from the significant disparity in material properties between the carbon fibre
101 and resin in CFRP. Current research on hybrid machining methods, which combines
102 EDM and traditional machining, primarily focuses on electrical discharge-mechanical
103 hybrid grinding [23,24]. During hybrid grinding, arc plasma generated by EDM thermally
104 removes the surface material of the workpiece, while softening the remaining
105 unremoved material to make it easy to remove by subsequent mechanical grinding [25].
106 Such a hybrid machining method enables high-precision machining of high-hardness
107 materials [26]. However, to the authors' knowledge, there are currently no reports on the
108 combination of EDM and mechanical processing to address the machining challenges
109 of multilayer composites such as CFRP, which have significant anisotropy and
110 inhomogeneity.

111 In this study, to address the challenges of achieving high-quality and high-
112 efficiency machining of deep micro-holes in CFRP, an electrical discharge-mechanical
113 hybrid drilling method was proposed based on an in-depth understanding of the
114 microstructure of the CFRP material. First, the principle of electrical discharge-
115 mechanical hybrid drilling was described to show the theoretical foundations of this
116 method for solving the challenges of CFRP micro-hole machining. Then, high-speed

117 photography, processing debris analysis, discharge state monitoring, and finite element
118 simulation for temperature distribution were performed to investigate the machining
119 process and material removal mechanism of this hybrid drilling process. Finally, the
120 machining efficiency, machining quality, and tool electrode wear of this hybrid drilling
121 in machining CFRP micro-holes were comprehensively investigated and compared
122 with those of EDM in machining CFRP micro-holes to demonstrate the feasibility and
123 advantages of the hybrid drilling.

124 The electrical discharge-mechanical hybrid drilling method proposed in this study
125 combines the advantages of EDM and mechanical drilling, providing a new solution
126 for micro-machining of multi-layer composite materials with significant anisotropy and
127 inhomogeneity. These multi-layer composites are difficult to process effectively using
128 a single process method due to the large differences in their internal material properties.
129 For example, in CFRP, the properties of carbon fibre and resin differ significantly, with
130 the high hardness of carbon fibre and the non-conductive nature of the resin posing
131 challenges for both mechanical drilling and EDM. The proposed hybrid drilling method
132 ingeniously exploits the significant difference in conductivity between carbon fibre and
133 resin in CFRP, enabling electrical discharge machining and mechanical drilling to work
134 together effectively. Statistical results indicate that developed hybrid drilling method
135 for machining deep micro-holes on CFRP offer significant advantages over
136 conventional mechanical drilling and non-conventional manufacturing such as EDM,
137 laser machining, and AWJM (Fig. 1). This hybrid drilling method is also applicable to
138 the micro-hole machining of other composite materials with similar systems to CFRP,
139 such as carbon fibre reinforced polyamide (CF/PA) and carbon fibre reinforced
140 polyether ether ketone (CF/PEEK), as demonstrated in Appendix 1.

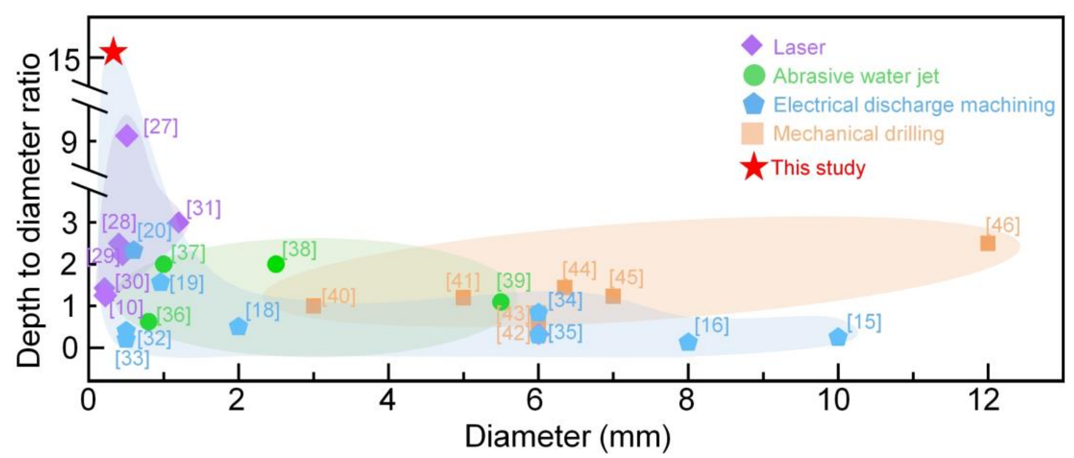


Fig. 1. Current status of hole machining in CFRP.

141 ## 2. Principle of electrical discharge-mechanical hybrid drilling

142 Fig. 2 shows a schematic of a widely used plain CFRP (Fig. 2a) and a typical
143 localised microstructure (Fig. 2b) observed via scanning electron microscopy (SEM),
144 in which the resin and carbon fibre appear in alternating layers. Woven carbon fibre
145 cloth is impregnated with resin and cured to form CFRP material. In the industry,
146 secondary processing of CFRP parts is typically performed perpendicular to the carbon
147 fibre layers. It is inevitable to remove the carbon fibre and resin layers alternately when
148 machining micro-holes in CFRP. A carbon fibre layer with high hardness and a resin
149 layer with non-conductive properties hinder the feasibility of mechanical drilling and
150 EDM for the high-quality machining of CFRP deep micro-holes, respectively.

151 In this study, a novel machining method called electrical discharge-mechanical
152 hybrid drilling method was proposed to integrate the advantages of EDM and
153 mechanical drilling. In this method, a tungsten steel drill with high-speed rotation is
154 used as the tool electrode, EDM and mechanical drilling are performed effectively to
155 remove the carbon fibre and resin layers, respectively. A pulse voltage is applied
156 between the tool electrode and workpiece at all times during machining. The gap
157 voltage is monitored, and the tool electrode feed is controlled using a special servo-
158 control strategy to enable accurate utilizing EDM and mechanical drilling. This
159 specialized servo control strategy functions efficiently owing to the distinct difference
160 in electrical conductivity between the carbon fibre and the resin in CFRP.

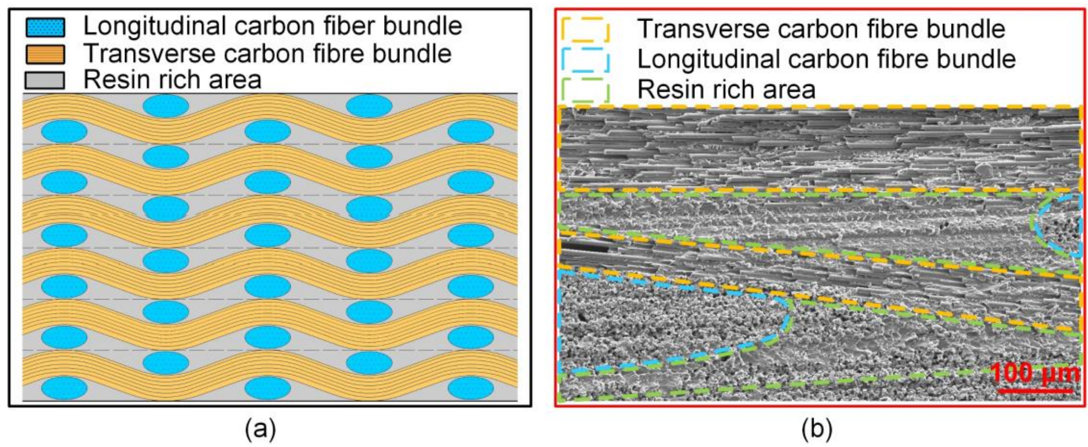


Fig. 2. Microstructure of CFRP. (a) Schematic diagram of the CFRP microstructure. (b) SEM micrograph of the CFRP.

161 **2.1 Servo feed control strategy for tool electrode**

162 During the electrical discharge-mechanical hybrid drilling of a CFRP, the gap
163 voltage waveforms can be classified into three types: open-circuit, spark discharge, and
164 short-circuit waveforms (Fig. 3a). It is worth emphasising that the gap voltage
165 waveforms in the short-circuit and arc discharge states are difficult to distinguish owing
166 to the relatively high resistivity of CFRP [35]. Meanwhile, the spindle servo motions
167 corresponding to both the short circuit and arc discharge are fast retractions; thus, the
168 arc discharge waveform is not described herein. As shown in Fig. 3b, the voltage signals
169 between the electrodes are collected periodically, and the average gap voltage U is
170 calculated during the machining process. The average voltage is defined as the
171 arithmetic average of the voltage signals continuously collected during a specific time
172 period, which is calculated by summing all voltage measurements during that time
173 period and dividing them by the total duration of that time period. This process
174 effectively reflects the average performance of the voltage signal over that period. The
175 average gap voltage U corresponding to the open-circuit, spark discharge, and short-
176 circuit states decreases in steps. Thus, the average gap voltage U can be used to
177 determine the machining state, which in turn determines the spindle motion state.

178 Fig. 3c shows the specific servo-control process for the spindle motion. The
179 machining depth L is set before the start of machining, and the high-voltage threshold
180 U_H and low-voltage threshold U_L are set according to the specific machining conditions.
181 During machining, the average gap voltage U is compared with U_H and U_L to determine

182 the current gap voltage waveform. When the gap voltage waveform is in the open-
183 circuit, spark discharge, and short-circuit states, the spindle feeds forwards rapidly,
184 feeds slowly, and retracts rapidly, respectively.

185 When processing the conductive carbon fibre, servo control based on the gap
186 voltage waveform maintains a stable spark discharge state between the electrodes, thus
187 ensuring a reliable EDM of the carbon fibre layer. When machining the resin layer, the
188 gap voltage waveform is maintained in an open-circuit state owing to the non-
189 conductive properties of the resin. Thus, a high-speed rotating tool electrode is
190 continuously and rapidly fed to mechanically machine the resin layer. Due to the
191 significant difference in the electrical conductivity of carbon fibre and resin, the servo
192 control strategy used in this study can fully utilize EDM to remove high hardness
193 carbon fibre and mechanical drilling to remove non-conductive resin, integrating the
194 advantages of EDM and mechanical drilling. This provides an effective approach for
195 achieving high-quality and efficient machining of deep micro-hole in CFRP.
196 Machining is completed when the machining state is an open-circuit state and the
197 machining depth reaches the set depth L. It is important to emphasize that the servo
198 feed control strategy leverages the significant difference in electrical conductivity
199 between resin and carbon fibre. As a result, this strategy remains effective regardless of
200 the distribution of carbon fibre and resin within the CFRP material. This implies that
201 the weaving method of CFRP and the location of hole machining have no significant
202 impact on the effectiveness of the servo control strategy.

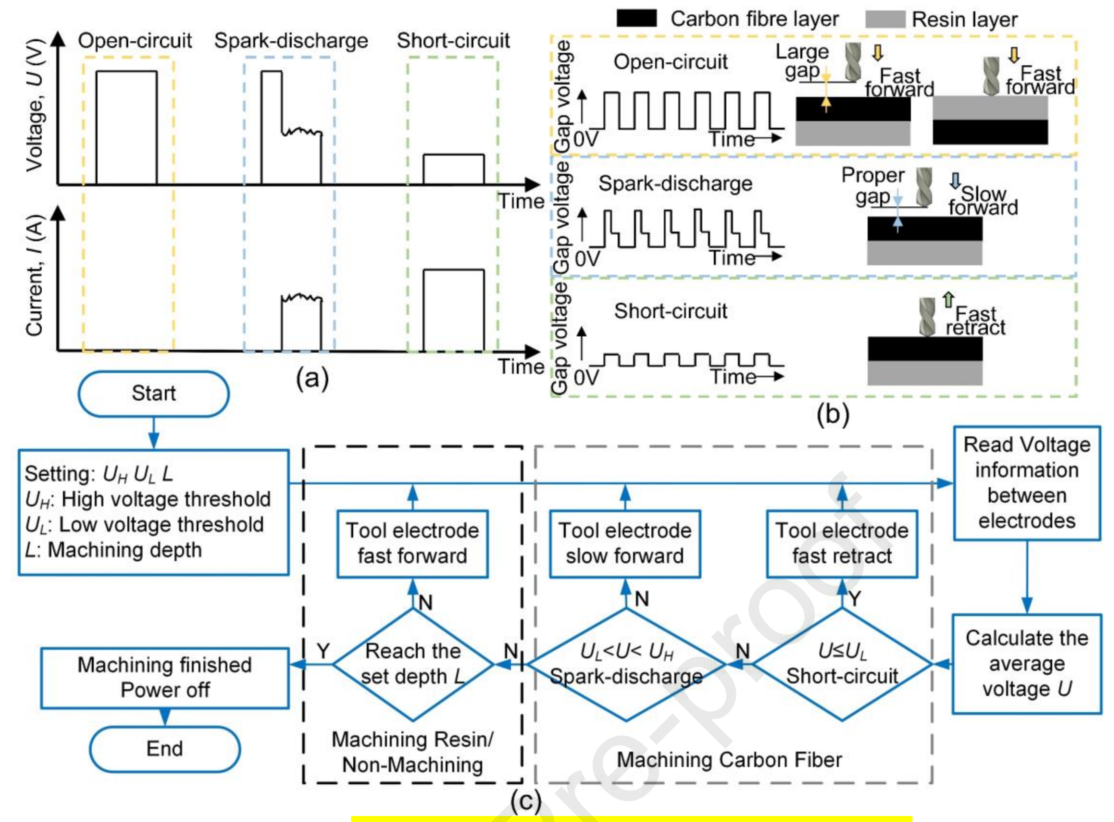


Fig. 3. Servo control during electrical discharge-mechanical hybrid drilling of a CFRP. (a) Theoretical voltage and current waveforms during hybrid machining. (b) Principle of servo-feed control. (c) Servo-control process during EDM.

203 Fig. 4 illustrates an example of the material removal process to better explain the
204 servo feed control strategy during hybrid drilling of CFRP. Along the tool electrode's
205 feed direction, the carbon fibre and resin are not distributed in a uniformly alternating
206 pattern (Fig.4 (a)). When the tool electrode is close to the machining surface, discharge
207 breakdown occurs in the carbon fibre area due to the good electrical conductivity of the
208 carbon fibre, resulting in the removal of the carbon fibre by EDM (Fig. 4b). Meanwhile,
209 a small amount of resin material next to the carbon fibre is removed by the high
210 temperature generated by the discharge (Fig. 4c). In this stage, based on a servo control
211 strategy, the tool electrode moves slowly forward to maintain a stable inter-electrode
212 gap. As the tool electrode is fed forward, the resin in the processing area that has not
213 been thermally removed is removed through mechanical drilling. EDM of carbon fibre
214 is carried out simultaneously with the mechanical drilling of the remaining resin (Fig.
215 4d). The distribution of carbon fibre and resin does not significantly affect the
216 integration of the advantages of EDM and mechanical drilling during hybrid drilling.
217 This explains why the effectiveness of the servo feed control strategy remains

218 unaffected by the weaving method or the hole machining position of the CFRP.

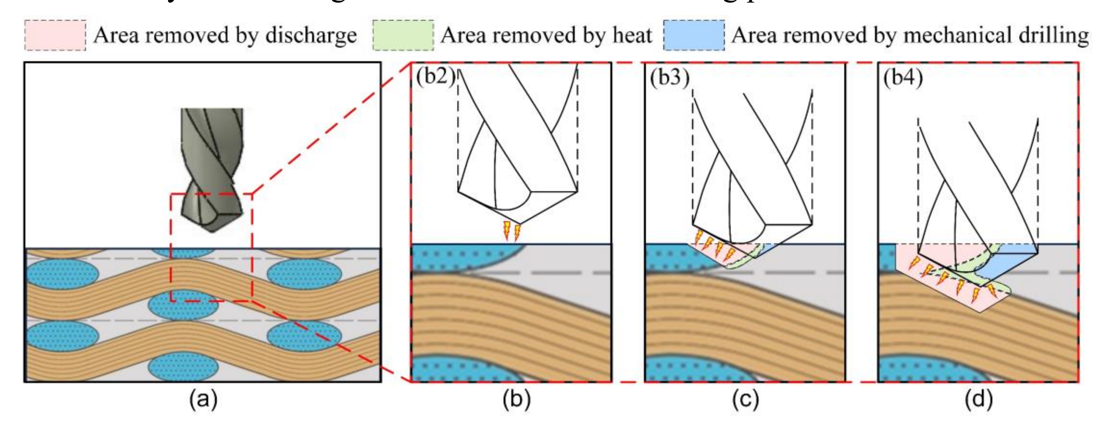


Fig. 4. Schematic diagram of the material removal process during CFRP hybrid drilling. (a) Machining position. (b) The case of removal only by electrical discharge. (c) The case of removal by electrical discharge and heat. (d) The case of removal by discharge, heat and mechanical drilling.

219 **2.2 Material removal process**

220 Fig. 5 shows the four stages of the electrical discharge-mechanical hybrid drilling
221 of CFRP: carbon fibre machining, carbon fibre layer-to-resin layer transition machining,
222 resin layer machining, and resin layer-to-carbon fibre layer transition machining. The
223 detailed machining process is described below. Based on the observed cross-section
224 structure of the CFRP material (Fig. 2), the material distribution inside the CFRP is
225 simplified to a uniform periodic alternation of carbon fibre and resin layer, which
226 facilitates the clear illustration of the material removal process.

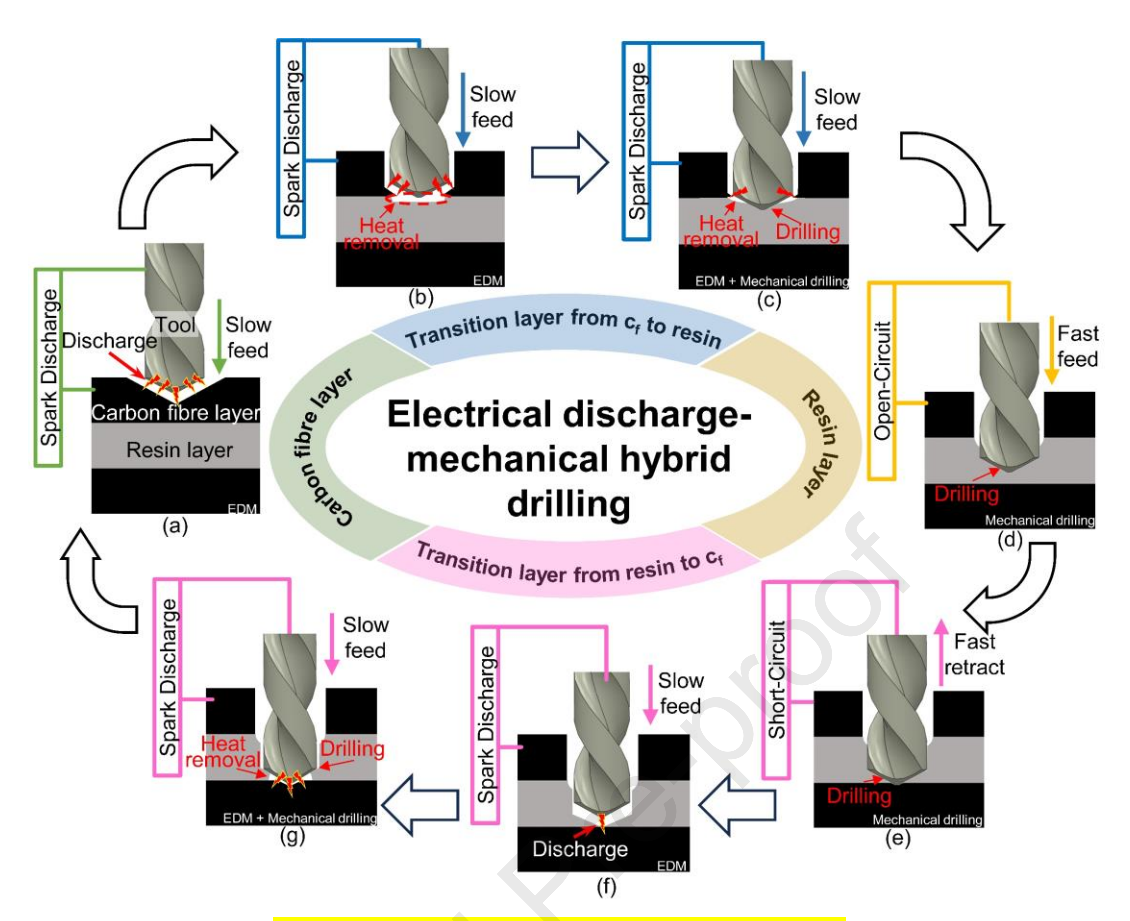


Fig. 5. Principle of electrical discharge-mechanical hybrid drilling. (a) Machining of the carbon fibre layer. (b) The start of transition layer machining from carbon fibre layer to resin layer. (c) The end of transition layer machining from carbon fibre layer to resin layer. (d) Machining of the resin layer. (e) The moment when the tool electrode comes into contact with the carbon fibre and rapidly retract. (f) The start of transition layer machining from resin layer to carbon fibre layer. (g) The end of transition layer machining from resin layer to carbon fibre layer.

227 As shown in Fig. 5a, when machining the carbon fibre layer, a continuous spark
228 discharge is generated between the tool electrode and the workpiece because of the
229 conductive carbon fibre. EDM is performed to remove the carbon fibre layer. Most of
230 the gap voltage waveforms are spark-discharge states owing to the servo-control
231 strategy described above to ensure EDM stability. Once the tool electrode touches the
232 workpiece, it quickly retracts owing to the detection of a short circuit. Thus, the carbon
233 fibre layer is machined using only EDM, which avoids wear and breakage of the tool
234 electrode because of mechanical drilling.

235 Fig. 5b shows the machining of the transition layer from the carbon fibre layer to
236 the resin layer. The resin close to the carbon fibre layer can be removed by the heat
237 generated from the discharge of the carbon fibre. As the high-speed rotating spindle
238 feeds, the resin that is not removed by heating is removed by mechanical drilling. Both

239 EDM and mechanical drilling are performed simultaneously during this stage (Fig. 5c).
240 Fig. 5d shows the machining principle of the resin layer. The gap voltage waveform
241 maintains an open-circuit state at this stage owing to the electrical insulation of the resin.
242 Thus, a tool electrode with high-speed rotation is fed rapidly (Fig. 3b). Mechanical
243 drilling is performed to remove the resin layer effectively until the end of the resin layer
244 machining.
245 As the tool electrode continues to feed, when the tip of the tool electrode touches
246 the next carbon fibre layer, it automatically retracts because a short circuit is detected
247 (Fig. 5e). EDM is then steadily performed via servo control to remove the carbon fibre.
248 This area represents the transition from the resin to the carbon fibre layer. As shown in
249 Fig. 5f, the resin close to the carbon fibre layer is thermally removed owing to the
250 discharge between the tool electrode and carbon fibre layer. Subsequently, the resin that
251 is not removed by the heat is removed by mechanical drilling as the tool electrode
252 continues to be fed. Both EDM and mechanical drilling are performed simultaneously
253 until the bottom of the tool electrode is completely inside the carbon fibre layer (Fig.
254 5g). Owing to the characteristics of alternating lamination of the carbon fibre and resin
255 in the CFRP, the above four stages are performed alternately to achieve high-quality
256 machining of the CFRP micro-holes.
257 As indicated by the above analysis, all carbon fibre layers are thermally removed
258 by EDM during the electrical discharge-mechanical hybrid drilling of the CFRP (Fig.
259 6a). The removal mechanism of the resin layer is illustrated in Fig. 6b, which can be
260 divided into three parts. The top part (i) and bottom part (iii) of the resin are removed
261 by both mechanical drilling and thermal effects, because they are close to the carbon
262 fibre layer, and the middle part of the resin (ii) is removed only by mechanical drilling.

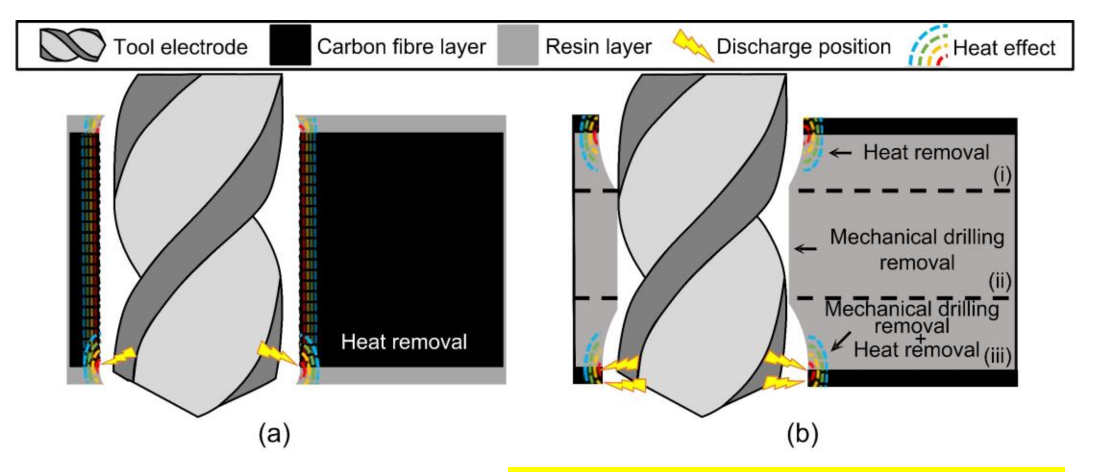


Fig. 6. Mechanism of material removal in electrical discharge-mechanical hybrid drilling of CFRP. (a) Removal mechanism of carbon fibre in the CFRP. (b) Removal mechanism of resin in the CFRP.

263 In the actual CFRP hole machining process, the carbon fibre and resin layers may
264 not be removed alternately, as this depends on the weaving method of the material itself
265 and the specific location of the hole. However, during the hybrid drilling of CFRP holes,
266 the removal of carbon fibre by EDM and the removal of resin by mechanical drilling
267 can be carried out either alternately or simultaneously. The developed hybrid drilling
268 method is effective for all variations of carbon fibre and resin distribution in CFRP (Fig.
269 4). Additionally, the switching between EDM and mechanical drilling, controlled by
270 the servo strategy, depends on the spatial distribution of carbon fibre and resin within
271 the processing area and does not follow a fixed switching frequency.

272 3. Material and methods

273 3.1 Material characteristics

274 A plain CFRP with dimensions of 50 mm × 10 mm × 5 mm was utilized for the
275 experiments, in which the reinforcing phase was high-strength carbon fibre T700SC-
276 12K (7 μm in diameter) and the matrix phase was an epoxy resin with thermosetting
277 properties. The chemical structure of the resin remains stable at room temperature.
278 However, when the temperature exceeds its decomposition threshold, the resin
279 undergoes thermal degradation, leading to its conversion into gaseous products. The
280 material properties of the CFRP are detailed in Table 1. There is a significant difference
281 between carbon fibre and epoxy resin in terms of thermal conductivity and electrical
282 resistivity, which leads to the non-homogeneity of the CFRP. Meanwhile, the thermal

283 conductivity and electrical resistivity of carbon fibre differ in different directions,
284 resulting in anisotropy of the material.

285 Table 1. Material properties of CFRP [47,48]

	Carbon fibre	Resin
Resistivity [Ω·cm]	1.53×10^{-3}(Axial)/ 1.53×10^{-2} (Radial)	10^{16}~10^{17}
Thermal conductivity [$W\cdot m^{-1}\cdot K^{-1}$]	50 (Axial)/5 (Radial)	0.2
Specific heat [J/(Kg·K)]	1884	710
Density [$Kg\cdot m^{-3}$]	1850	1250
Thermal decomposition [K]	-	693
Boiling point [K]	-	800
Sublimation point [K]	3923	-

286 **3.2 Experimental procedures**

287 **3.2.1 Machining equipment**

288 Fig. 7 shows the self-developed machining device. A three-phase stepping motor
289 with a resolution of 0.1 μm was used for micro-step driving. The tool electrode was
290 driven by a high-speed electric spindle (BM-320, NAKANISHI). When clamping the
291 tool electrode, the spindle and the electrode must be insulated to avoid the interference
292 from high-frequency signals and currents. The pulse voltage used for machining was
293 the output by a transistor pulse power supply.

294 To clarify the machining mechanism of the electrical discharge-mechanical hybrid
295 drilling, a pico-oscilloscope (Pico-5000D, TEKTRONIX) and high-speed camera
296 (VEO-710, PHANTOM) were used to monitor the gap voltage waveform and observe
297 the gap phenomenon, respectively. The machining process was conducted at the edge
298 of the workpiece to ensure that the hole wall discharge could be clearly captured by the
299 high-speed camera (Fig. 7(a)). Spindle movement was controlled using the servo-
300 control system. The processing conditions for the observation and machining are listed
301 in Table 2. The open circuit voltage was set to 110V and the duty cycle of the pulse
302 power supply was 50%. When the average voltage between the electrodes is higher than
303 the high voltage threshold U_H, the state is judged to be open-circuit state; when it is
304 lower than the low voltage threshold U_L, the discharge state is the short-circuit; And
305 others are the spark discharge state. The peak discharge current is 1.8A. The electrode
306 rotation speed is 3500 rpm.

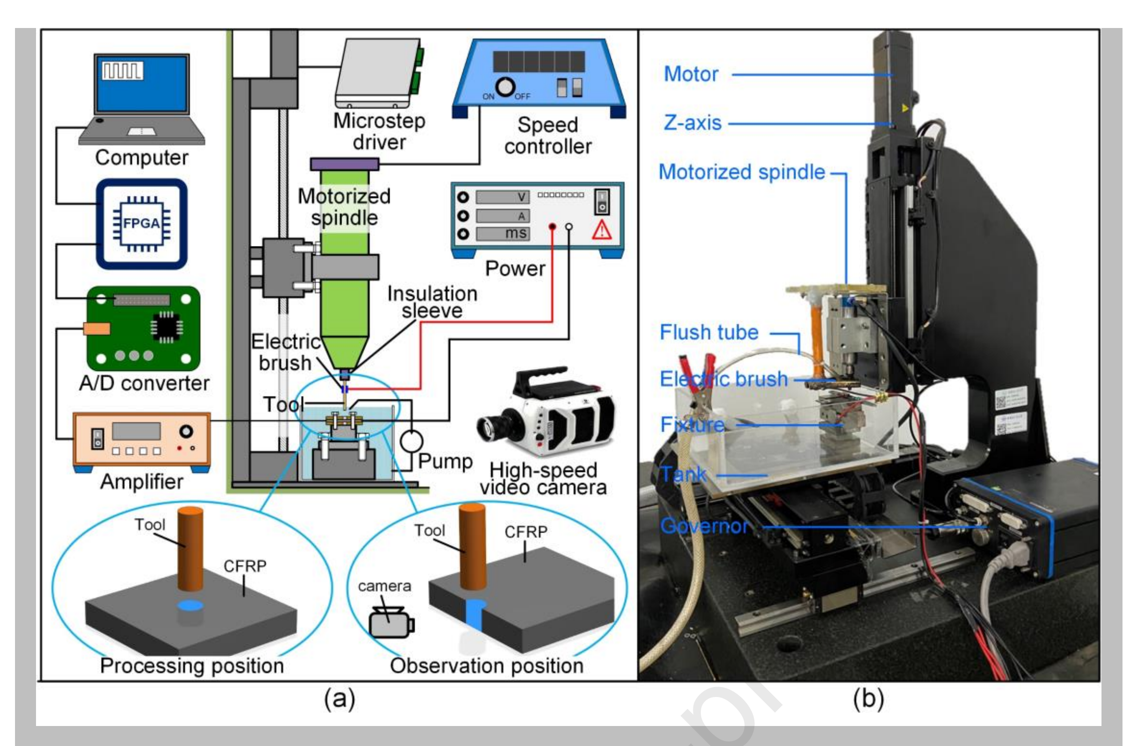


Fig. 7. Machining experiment setup. (a) Schematic diagram of the experimental setup. (b) Experimental platform.

307 Table 2. Experimental conditions

Parameters	**Value**
Open voltage (V)	110
Peak discharge current (A)	1.8
Pulse frequency (kHz)	50
Duty ratio (%)	50
Workpiece	CFRP
Polarity	Workpiece (+); Tool electrode (-)
Electrode rotation speed (rpm)	3000
High voltage threshold (V)	50
Low voltage threshold (V)	13

308 **3.2.2 Micro-hole machining experiments**

309 To demonstrate the feasibility and advantages of the electrical discharge-
310 mechanical hybrid drilling method, micro-hole machining experiments were conducted
311 on the CFRP with a thickness of 5 mm using the developed machining equipment (Fig.
312 7). The micro-hole machining experiment was conducted at the centre of the workpiece,
313 differing from the observation experiment which was conducted at the edge. The
314 machining efficiency, tool electrode wear, and machining quality of the electrical
315 discharge-mechanical hybrid drilling for CFRP micro-holes were systematically
316 analysed and compared with those of EDM. The working medium was deionised water,
317 and immersion fluid machining was used for the experiments. A tungsten steel drill and

318 tungsten steel drill without tool tip were used as tool electrodes in the hybrid drilling
319 (Fig. 8a) and EDM (Fig. 8b), respectively. The tungsten steel drill tool electrode shown
320 in Fig. 8(a) was a directly procured ready product. These microfine drills have
321 established applications in the market, and their hardness, wear resistance, and
322 dimensional accuracy satisfy the processing requirements of this study. In contrast, the
323 tungsten steel drill without tool tip used for the control experiment (Fig. 8(b)) was
324 customised according to the experimental requirements. The same tungsten steel drill
325 bit shown in Fig. 8(a) was used as the base material, and the tool tip of the drill was
326 carefully removed using high-precision wire electrical discharge machining (WEDM)
327 to obtain the non-main-cutting-edge form. This ensured the rigor of the control
328 experiments by maintaining consistent material properties and structural between the
329 two tool electrodes, except for the differences in the main cutting edge.

330 There was no mechanical drilling process because the tool electrode did not have
331 the main cutting edge when machining micro-holes using EDM. The material properties
332 of the tungsten steel drills are presented in Table 3. After the micro-hole machining, a
333 SEM (HITACHI SU8010) and a laser scanning confocal microscope (OLS3000,
334 OLYMPUS) were used to observe the morphology and contour of the machined hole.

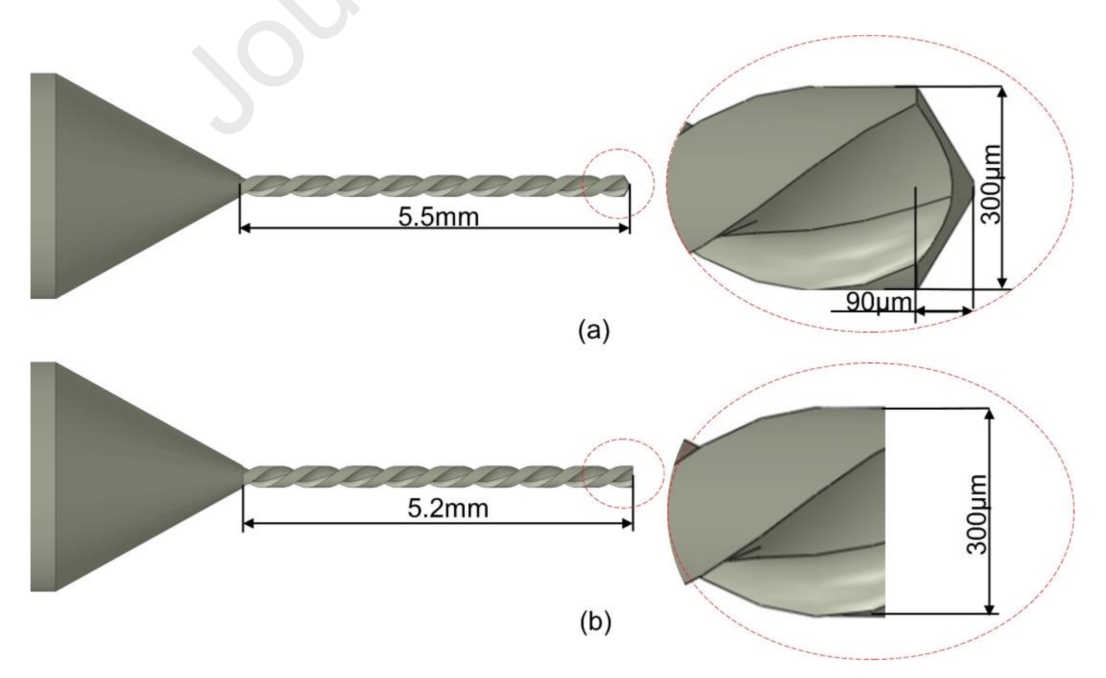


Fig. 8. Tool electrodes. (a) Tungsten steel drill. (b) Tungsten steel drill without tool tip.

335 Table 3. Material properties of tungsten steel drill (tungsten steel: T5)

Parameters	Value
Resistivity (Ω·cm)	5×10^{-6}
Thermal conductivity ($W\cdot m^{-1}\cdot K^{-1}$)	65
Density ($Kg\cdot m^{-3}$)	1.4×10^{4}
Melting point (K)	1773
Boiling point (K)	5800

336 **3.3 Simulation for mechanism analysis**

337 During the electrical discharge-mechanical hybrid drilling of CFRP, it is difficult
338 to clearly observe the removal of material from the transition layer between the carbon
339 fibre and resin owing to the small size of this area. Thus, a transient temperature finite
340 element model (FEM) was developed to investigate the temperature evolution of the
341 transition layer during the hybrid drilling process. The thermal effects of the arc plasma
342 generated by the discharge of carbon fibre during hybrid drilling were quantitatively
343 analysed and discussed. This can be used to reveal the mechanisms of material removal
344 from the transition layer.

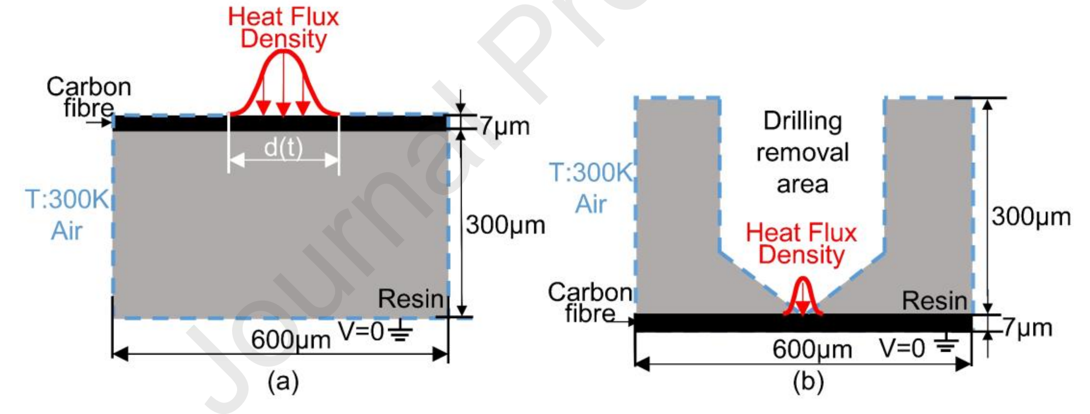


Fig. 9. Simulation of transition layer machining. (a) Transition from the carbon to resin layer. (b) Transition from the resin to carbon layer.

345 Fig. 9 shows the simulation model. The thickness of carbon fibre layers in the
346 model was set to 7μm, which was consistent with the diameter of carbon fibre in the
347 actual CFRP. Table 1 lists the material properties. The axial and radial thermal
348 conductivities of the carbon fibre were set as 50 W/(m·K) and 5 W/(m·K), respectively,
349 considering the anisotropy of the material. The simulation model was 600 μm in length
350 and 307 μm in thickness (resin layer: 300 μm; carbon fibre layer: 7 μm), and 1/4 of the
351 simulation model was taken for calculation. The circular area with a time-dependent
352 diameter $d(t)$ at the centre of the discharge surface of the workpiece was the energy
353 input region where the heat flux q was exerted. Except for the energy input region, all

354 other surfaces were considered to exchange heat with air (air temperature T = 300 K,
355 and convective heat exchange coefficient h_c = 15 W/(m^2·K)). The electrical potential V
356 at the bottom surface of the workpiece was set as zero (ground level). The simulation
357 conditions were the same as those of the actual machining conditions listed in Table 2.
358 In addition, although the open circuit voltage is 110V, the energy of the plasma is mainly
359 determined by the sustain voltage, and it is necessary to measure its actual sustaining
360 voltage and apply it to simulation calculations. The discharge sustain voltage during
361 CFRP processing can be determined to be 18V by measuring the discharge waveform
362 during machining.

363 To simplify the simulation calculations, the following assumptions were made for
364 the model. (1) All material properties are dependent on temperature. However, there is
365 an extreme lack of information on CFRP material properties with thousands of degrees
366 of freedom. Therefore, the relationship between the material properties and temperature
367 was not considered in the simulation. (2) Only the heat conduction process of the CFRP
368 was considered in the simulation of the CFRP discharge process, while the material
369 removal process of the CFRP resulting from vaporisation was not taken into
370 consideration.

371 Circular Gaussian heat sources are widely used to simulate the heat flux of plasma
372 channels during EDM [49]. Therefore, in this study, a Gaussian heat source with a time-
373 varying diameter was used as the applied energy, and the heat flow density was
374 calculated using the following equation:

$$q(r,t) = q_m(t)\, exp(\frac{-kr^2}{\frac{d^2(t)}{4}}) \tag{1}$$

375 where r is the radius of the cylindrical plasma channel, $q(r, t)$ is the heat flow density at
376 radius r and time t, $q_m(t)$ is the heat flux density at the centre of the plasma channel at
377 time t, k is the heat source concentration factor, where k takes the value of 4.5[49], and
378 $d(t)$ is the time-dependent diameter of the arc plasma, which is determined by observing
379 the plasma diameter as a function of time under simulation conditions using a high-
380 speed camera.

381 The heat flux density $q_m(t)$ at the centre of the arc column can be obtained by

382 calculating the discharge power *Q(t)* in Eq. (1), as expressed in Eq. (2).

$$Q(t) = \eta u(t)i(t) = \int_0^{\frac{d(t)}{2}} q(r,t)2\pi r dr \tag{2}$$

383 where η is the ratio of discharge energy distribution at the anode and has a value of 0.4
384 according to Xia's study [50], *u(t)* is the discharge voltage and is equal to 18 V, and *i(t)*
385 is the discharge current, which is obtained by a single discharge experiment under the
386 simulation conditions.

387 An expression for the heat flux density at the centre of the arc column can be found
388 based on Eq. (2), as shown in Eq. (3):

$$q_m(t) = \frac{4.57\eta u(t)i}{\frac{\pi d^2(t)}{4}} \tag{3}$$

389 **4 Results and discussion**

390 **4.1 Mechanism analysis**

391 In this section, high-speed camera observation, processing debris analysis, and
392 finite element simulation of the temperature distribution were performed to investigate
393 the machining process and material removal mechanism of electrical discharge-
394 mechanical hybrid drilling.

395 **4.1.1 Observation of the electrical discharge-mechanical hybrid drilling process**

396 Observations of the hybrid drilling process are shown in Fig. 10. As clearly shown
397 in Figs. 10a and b, the three layers of material which are resin, carbon fibre and resin
398 layer were processed sequentially. The white dotted lines in Fig. 10 are the upper edges
399 of the CFRP workpiece. Fig. 10c shows that the spindle fed forwards rapidly owing to
400 the detection of an open circuit while machining the resin layer. Mechanical drilling
401 was performed to remove the resin layer effectively until the end of resin layer
402 machining. When machining the carbon fibre layer, a continuous spark discharge was
403 generated between the tool electrode and the workpiece owing to the electrically
404 conductive carbon fibre. Therefore, EDM was performed to remove the carbon fibre
405 layer (Fig. 10d). The dimensions of the discharge plasma in Fig. 10 appear unusually
406 large, primarily due to the unique properties of the CFRP material. The resin matrix in
407 CFRP is rapidly ablated during EDM due to its low thermal decomposition temperature,

408 resulting in a more intense combustion reaction that releases a large amount of energy
409 and light, causing the discharge plasma to appear larger. When the spindle continued to
410 feed, EDM switched to mechanical drilling as it processed the next layer of resin (Fig.
411 10e). Observations demonstrated that EDM and mechanical drilling can be accurately
412 used to remove material by monitoring the gap voltage waveform during hybrid drilling,
413 which integrates the advantages of both EDM and mechanical drilling. Moreover, the
414 gap voltage and current waveforms monitored during hybrid drilling can be utilized as
415 indicators for identifying the material removal process. Figs. 10(c) and 10(e) show that
416 the gap voltage and current waveforms are in the open-circuit state, indicating that the
417 tool electrode is rapidly moving forward to remove the resin via mechanical drilling.
418 While the gap voltage and current waveforms during the carbon fibre layer processing
419 exhibit a significant proportion of spark discharge states. The monitored gap waveform
420 is consistent with the observed gap phenomenon. Fig. 10 does not display all the gap
421 waveforms monitored during manufacturing, as the waveforms with excessively long
422 manufacturing times make it difficult to clearly identify the discharge status of
423 individual waveforms.

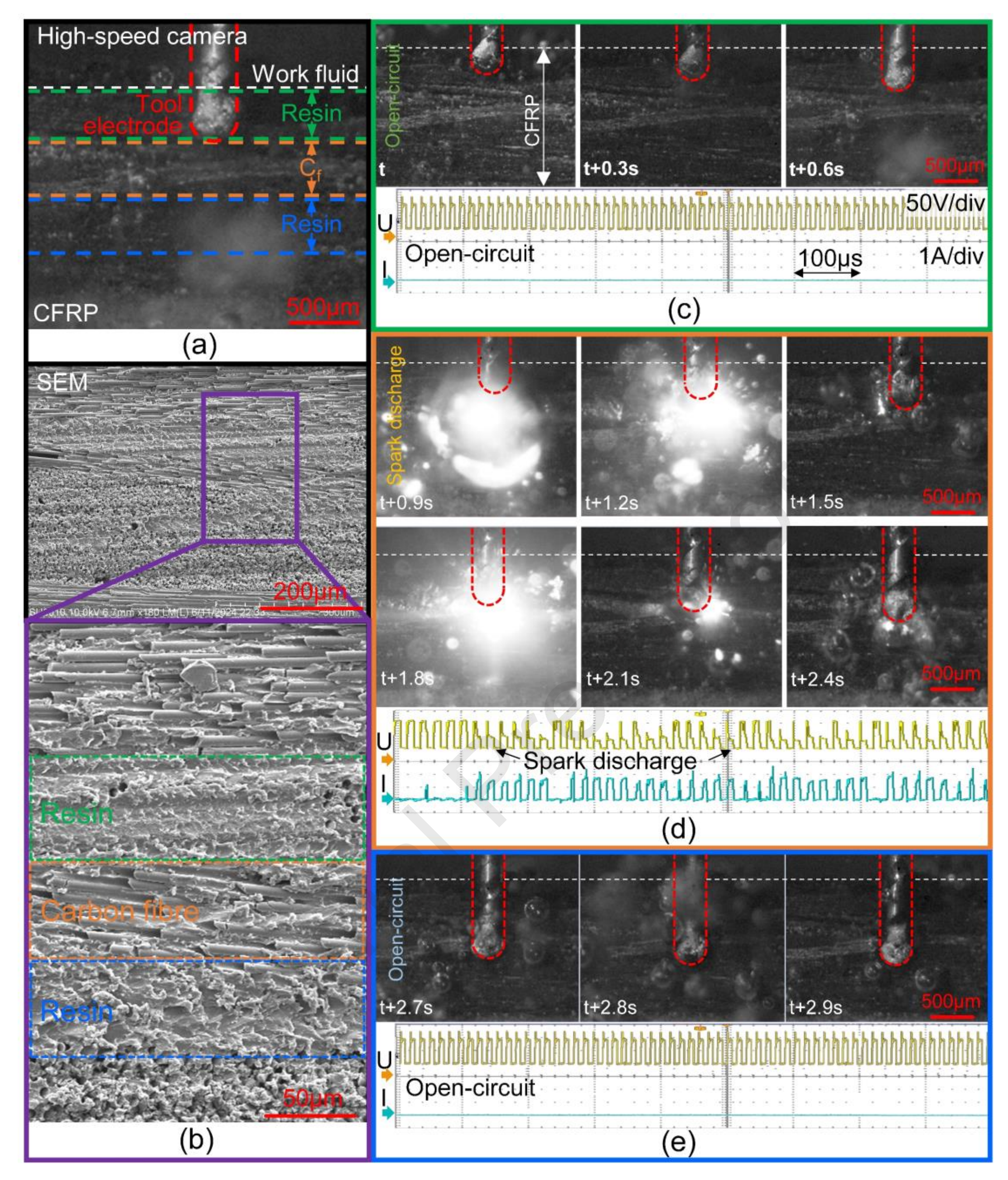


Fig. 10 Machining process observation using a high-speed camera. (a) Overall diagram of the tool electrode and workpiece in the machining area. (b) Partial enlargement of the workpiece. (c) The machining process and discharge waveforms of the resin layer. (d) The machining process and discharge waveforms of the carbon fibre layer. (e) The machining process and discharge waveforms of the next resin layer. The specific machining process can be seen in Supplementary Video 1.

424 **4.1.2 Machining mechanism of the carbon fibre layer**

425 Fig. 10 shows that the CFRP carbon fibre layer could be stably removed via EDM
426 during electrical discharge-mechanical hybrid drilling. Once the tool electrode touched
427 the workpiece, it quickly retracted owing to the detection of a short circuit. Therefore,

428 no mechanical drilling was performed at this stage. Furthermore, the debris produced
429 by electrical discharge-mechanical hybrid drilling was observed and compared with
430 that generated from the EDM and mechanical drilling processes to investigate the
431 removal mechanism of carbon fibre in depth.

432 Figs. 11a, b show the removal debris from the EDM of the CFRP and the debris
433 from CFRP drilling, respectively. Fig. 11c shows the debris produced by electrical
434 discharge-mechanical hybrid drilling, which consisted of both carbon fibre and resin
435 debris. To enhance the observation accuracy, a specialized sample preparation method
436 was adopted, in which the processed debris was finely adhered to the highly conductive
437 adhesive tape for SEM analysis. The cratering phenomenon shown in Fig. 11 was
438 thoroughly investigated and confirmed to be caused by tiny defects in the conductive
439 adhesive tape itself, rather than by removal products generated during the machining
440 process.

441 The comparison shows that the debris produced by mechanical drilling and that
442 produced by electrical discharge-mechanical hybrid drilling of the CFRP were
443 completely different (Fig. 11), proving that the carbon fibre was removed by EDM
444 during hybrid drilling. The morphology of debris generated from the hybrid drilling
445 was similar to that from EDM, but the carbon fibre debris was significantly smaller in
446 size. Fig. 12 shows the statistical results of the size of the carbon fibre debris produced
447 by different processing methods. EDM produced a significantly higher percentage of
448 carbon fibre debris with a length greater than 100μm than that of electrical discharge-
449 mechanical hybrid drilling. Larger debris sizes may lead to unstable discharge
450 conditions and poor machining quality.

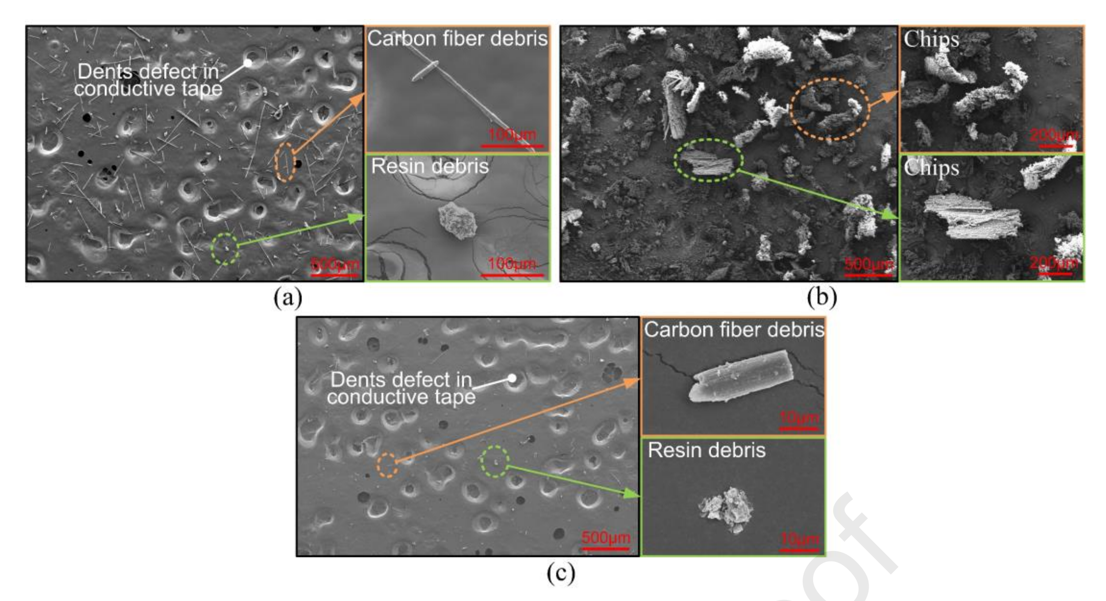


Fig. 11. Chips/debris of the CFRP removed by different machining methods. (a) Debris removed by EDM. (b) Chips removed by mechanical drilling. (c) Debris removed by electrical discharge-mechanical hybrid drilling.

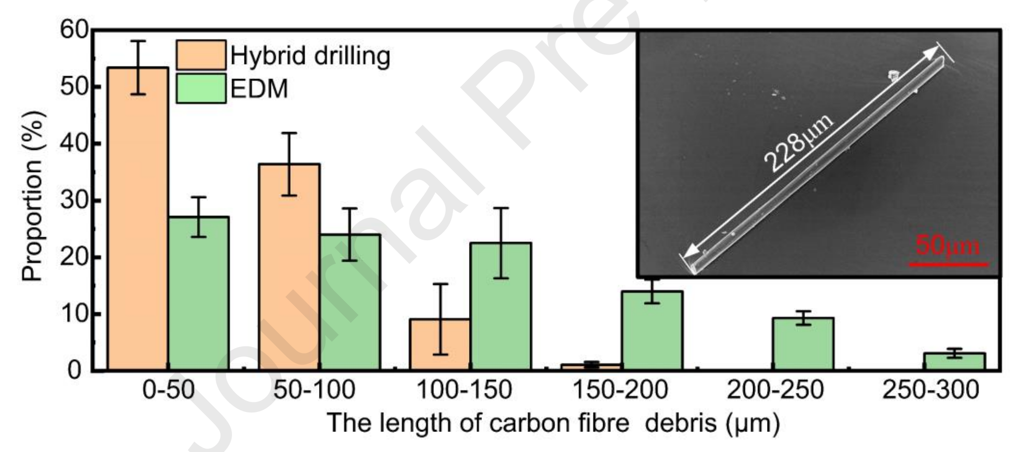


Fig. 12. Effect of different machining methods on the size of carbon fibre debris. The error bars represent the highest and lowest proportions of the number of carbon fibre debris of different lengths.

451 The reason for the larger size of the carbon fibre debris produced by EDM is
452 illustrated in Fig. 13a. In this study, the bottom surface of the tool electrode used for
453 EDM was parallel to the carbon fibre layer. Owing to the random discharge nature of
454 EDM, discharges may occur at two highly distant locations on a single carbon fibre,
455 causing the carbon fibre between the two discharge points to peel away from the
456 workpiece, thus producing long carbon fibre debris. However, a drill with tool tip was
457 used as the tool electrode during electrical discharge-mechanical hybrid drilling.
458 Because the bottom of the tool electrode had a conical structure, the discharge location
459 spread from the middle of the fibre layer to the surrounding ring, ensuring that discharge

460 occurred only at the exposed end of the carbon fibre (Fig. 13b). This prevented large
461 size carbon fibre spalling between two discharge points on a single carbon fibre, thereby
462 producing carbon fibre debris with smaller dimensions. The carbon fibre removal
463 process, as described in Fig. 13a, may also occur during electrical discharge-mechanical
464 hybrid drilling because the tool tip of the tool electrodes wear out over time. During the
465 discharge of CFRP, high-speed jets are injected into the gap, generating a jet force. The
466 carbon fibre at the point of discharge is hit by the high-speed jet in the direction
467 perpendicular to it, and then removed and flown away by the jet force in the direction
468 of the jet, as illustrated in Fig. 14 [51].

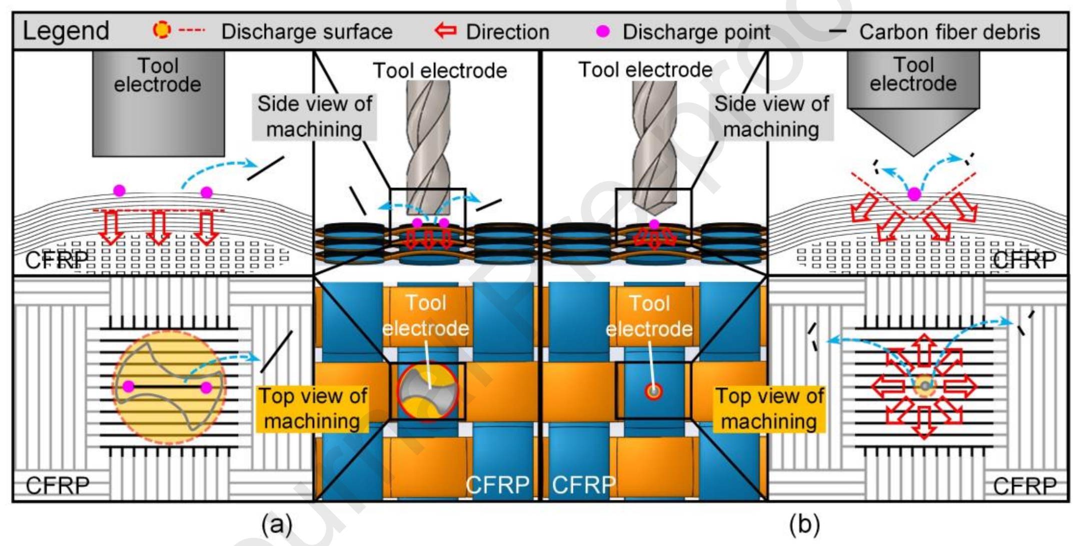


Fig. 13. Principle of machining methods influencing the size of carbon fibre debris. (a) EDM of the CFRP using a tool electrode without tool tip; large lengths of carbon fibre debris generated during EDM of the carbon fibre layer in the material. (b) Electrical discharge-mechanical hybrid drilling of the CFRP using tool electrodes with tool tip; small lengths of carbon fibre debris generated during EDM of carbon fibre layers in the material.

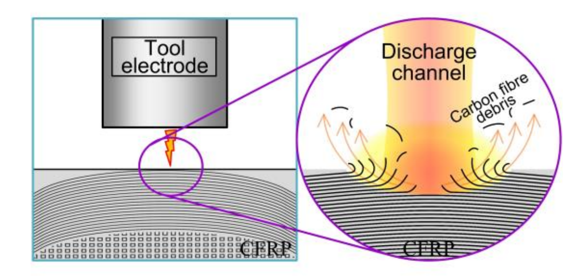


Fig. 14. Schematic of carbon fibre removed by the jetting force during EDM.

469 **4.1.3 Machining mechanism of the resin layer**

470 When machining the resin layer in electrical discharge-mechanical hybrid drilling,
471 the high-speed rotating drill bit feeds rapidly, owing to the detection of an open circuit.

472 Mechanical drilling was performed to effectively remove the resin layer. This is
473 demonstrated by the observations shown in Fig. 10.

474 Figs. 15a and b show the energy dispersive spectrometry (EDS) results of the
475 carbon fibre and resin debris obtained from hybrid drilling, respectively. To improve
476 the quality of the observations, gold was sprayed onto the debris before the observations
477 to enhance its conductivity, resulting in the presence of gold elements in the energy
478 spectrum. The energy spectrum of the carbon fibre debris showed only its own elements,
479 while elemental peaks not belonging to the resin element appeared in the debris, which
480 were confirmed to originate from the tool electrode. According to the principle of the
481 electrical discharge-mechanical hybrid drilling of the CFRP, most of the resin was
482 removed via mechanical drilling, and a small amount of resin near the carbon fibre layer
483 was removed by the thermal effect produced by EDM. The resin in the CFRP used for
484 machining was a thermosetting resin with a low thermal decomposition temperature,
485 which decomposes into CO and CO_2 owing to thermal effects during machining and
486 does not produce resin debris [48]. Thus, the resin debris containing the tool electrode
487 elements demonstrated that the resin layer of the CFRP was mainly removed by
488 mechanical drilling during hybrid drilling.

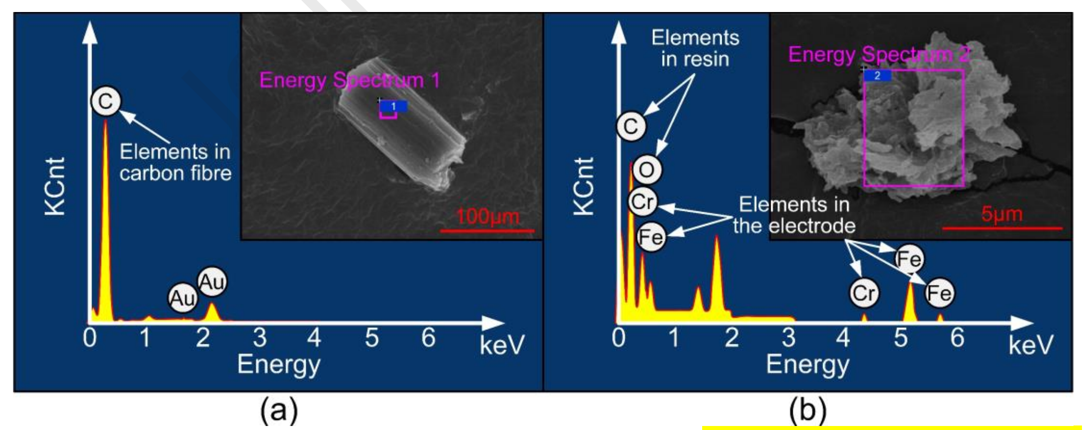


Fig. 15. Energy spectral analysis of debris produced by electrical discharge-mechanical hybrid drilling. (a) Carbon fibre debris. (b) Resin debris.

489 **4.1.4 Machining mechanism of the transition layer**

490 The resin in CFRP is a thermosetting resin that undergoes thermal decomposition
491 at temperatures above 693 K [48]. The heat transfer process from the carbon fibre to the
492 resin during the EDM process of the carbon fibre layer was obtained for quantitative
493 analysis of the heat removal of the resin. It can be used to investigate the proportions

494 of resin layer removed by heating and mechanical drilling respectively. Figs. 16a, b
495 show the simulation results of the transition layer from the carbon fibre layer to resin
496 layer and the transition layer from the resin layer to carbon fibre layer, respectively.
497 During the processing of the transition layer from the carbon fibre to resin layer, the
498 resin adjacent to the upper carbon fibre layer was removed owing to the thermal effect
499 generated by the discharge between the tool electrode and the carbon fibre (Fig. 16a).
500 Similarly, Fig. 16b shows that some of the resin exceeded the thermal decomposition
501 temperatures when processing the transition layer from the resin layer to carbon fibre
502 layer. The depth of thermal removal (h) of the resin increased with the increasing of
503 discharge energy during the EDM process. Resin that has not reached its thermal
504 decomposition temperature remains within the workpiece and is subsequently removed
505 through mechanical drilling. Wear experiments indicate that due to the low hardness of
506 the resin, the wear on the tool electrode during the mechanical drilling process is slight.
507 As the discharge energy increased, the proportion of thermally removed resin in the
508 transition layer increased, while the portion removed by mechanical drilling decreased.

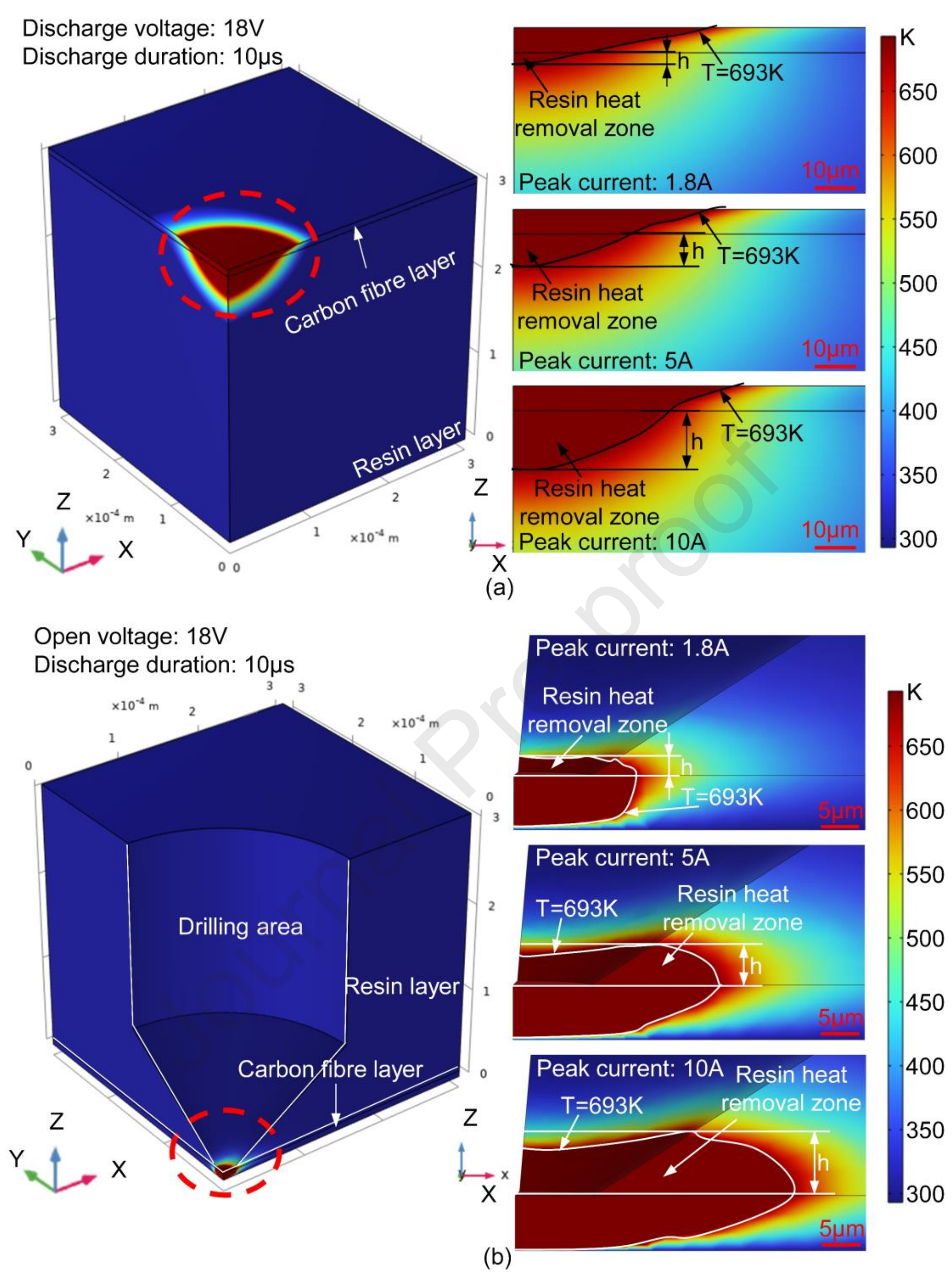


Fig. 16. Simulation of transition layer machining. (a) Transition from the carbon fibre to resin layers. (b) Transition from the resin to carbon fibre layers.

509 Fig. 17 shows the morphology of the hole profile machined by electrical discharge-
510 mechanical hybrid drilling. The surface morphology of the hole wall revealed periodic
511 variations, which were attributed to the different removal mechanisms of the resin and
512 carbon fibre layers during hybrid drilling. The diameter of the hole machined by EDM
513 was slightly larger than that of the tool electrode owing to the discharge gap, while the

514 diameter of the hole machined by mechanical drilling was similar to that of the tool.
515 During the electrical discharge-mechanical hybrid drilling of the CFRP, the carbon fibre
516 layer was removed by EDM, and the resin layer was removed by mechanical drilling.
517 Hence, the hole diameter of the carbon fibre layer was slightly larger. The experimental
518 results demonstrated that the carbon fibre and resin layers can be removed separately
519 by alternating EDM and mechanical drilling in the hybrid drilling process.

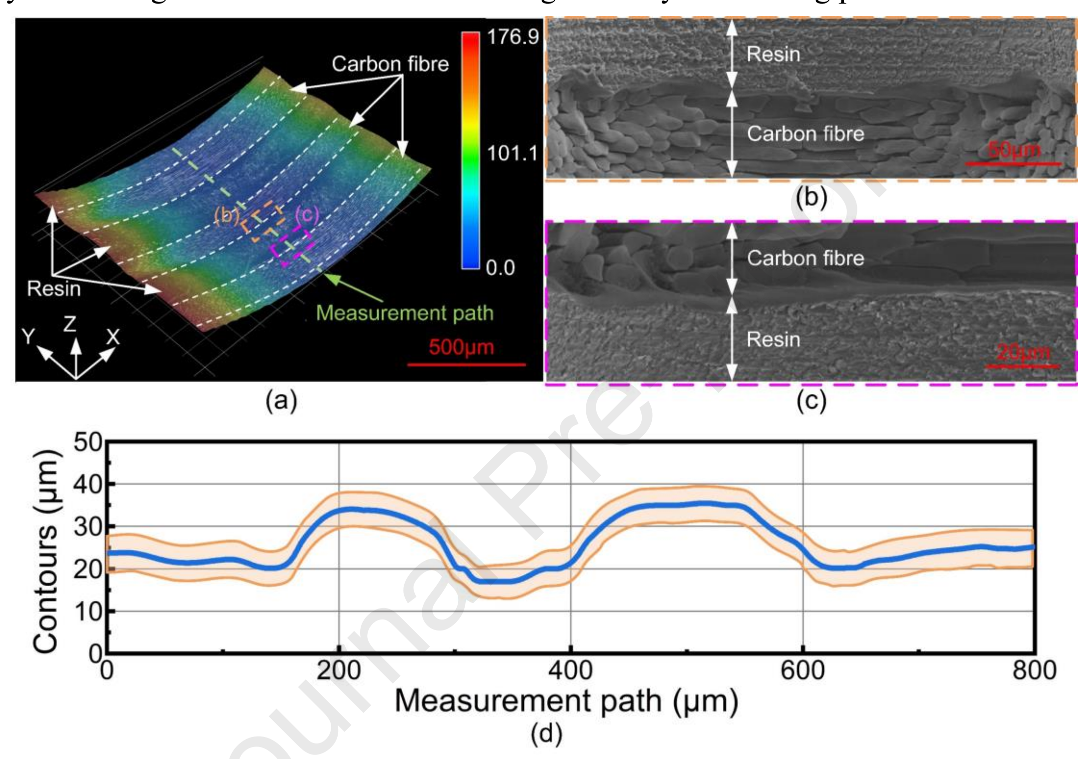


Fig. 17. Morphology of the machined hole profile. (a) Machined hole profile observed by laser confocal scanning microscopy. (b) The interface from resin to fibre. (c) The interface from fibre to resin. (d) The contour of the hole wall in the axial direction.

520 **4.2 Machining characteristics**

521 In this section, to reveal the machining characteristics of the electrical discharge-
522 mechanical hybrid drilling method, the machining efficiency, machining quality, and
523 tool electrode wear of through-holes machined using hybrid drilling method on CFRP
524 plates with thicknesses of 1 mm, 3 mm, and 5 mm are studied and compared with those
525 of EDM.

526 **4.2.1 Machining efficiency**

527 In this study, the material removal rate (MRR) was calculated by the following
528 methods: firstly, after the machining was completed, the inlet diameter, the outlet
529 diameter and the depth of machining of the hole were accurately measured;

530 subsequently, geometric calculations were carried out to obtain the actual volume of
531 material removed during the process; finally, specific MRR values were obtained by
532 dividing the removed volume by the processing time. Fig. 18 shows the machining
533 efficiencies of the different machining methods. The machining efficiency of electrical
534 discharge-mechanical hybrid drilling was significantly higher than that of EDM. The
535 machining efficiency of CFRP can be determined by combining the removal
536 efficiencies of the carbon fibre and resin layers, which are discussed separately below.

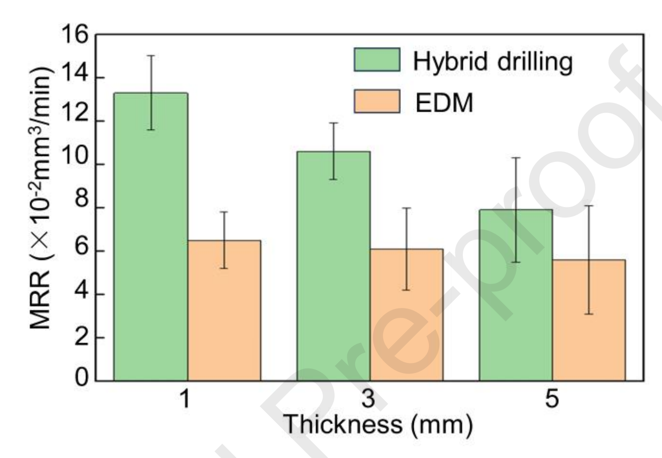


Fig. 18. Effect of different machining methods on machining efficiency. The error bars represent the highest and lowest material removal rates (MRR).

537 The CFRP carbon fibre layer is thermally removed by EDM during electrical
538 discharge-mechanical hybrid drilling, which is the same as EDM alone. The discharge
539 parameters for EDM and the hybrid drilling were the same in this study; therefore, the
540 discharge state was the main factor influencing the machining efficiency. Fig. 19 shows
541 the statistical results of the discharge state during the machining process of the carbon
542 fibre. The proportion of normal spark discharges was significantly higher in electrical
543 discharge-mechanical hybrid drilling than in EDM, while the short-circuit and open-
544 circuit states were significantly lower. This is attributed to the debris generated from
545 hybrid drilling was considerably smaller than that produced by EDM machining (Fig.
546 12), resulting in debris that was easier to remove from the discharge gap, thereby
547 ensuring a more optimal discharge state and enhanced machining efficiency.

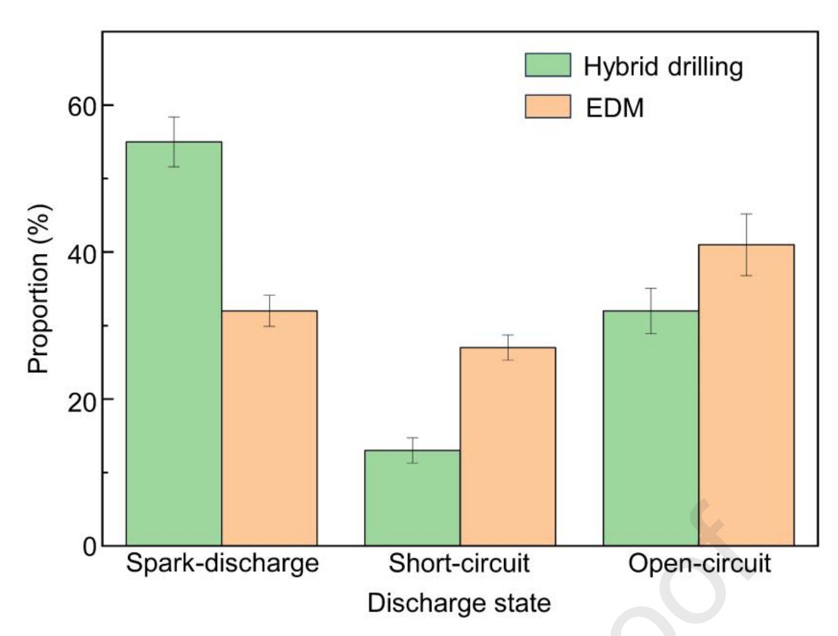


Fig. 19. Effect of different machining methods on the discharge state. The error bars represent the highest and lowest proportions of the different discharge states.

548 To machine the resin layer, the material was removed by mechanical drilling and
549 grinding during hybrid drilling and EDM, respectively. Mechanical drilling is a more
550 efficient process than grinding for machining holes in resin. Electrical discharge-
551 mechanical hybrid drilling exhibited a higher machining efficiency than EDM for both
552 the carbon fibre and resin layers. However, the difference in machining efficiency
553 between hybrid drilling and EDM decreased as the machining thickness increased (Fig.
554 18). This is because the materials of the tool electrodes (Tungsten steel drill) used in
555 the current experiments were not resistant to electrical erosion. The tool tip of the drill
556 bit gradually wears out during the hybrid drilling method, causing a reduction in
557 machining efficiency. This problem can be solved by replacing the drill bit material to
558 an electrically erosion-resistant material with a high melting point, thermal conductivity,
559 and electrical conductivity.

560 **4.2.2 Machining quality**

561 Fig. 20a shows a sectional view of the micro-holes produced by different
562 machining methods. According to the partial enlargement of Fig. 20a, the resin
563 impregnated in the carbon fibre layer undergoes intense thermal decomposition during
564 EDM, resulting in significant exposure of carbon fibre on the sidewalls of the micro-
565 hole. Meanwhile, the resin layer of the machined hole wall shows obvious non-flatness,
566 caused by the decomposition of the resin near the carbon fibre due to heat generated by

567 the discharge of the carbon fibre, thus causing the edges of the resin layer to be uneven.
568 In contrast, sidewalls of the micro-hole manufactured using hybrid drilling show better
569 surface integrity, with less exposed carbon fibre and a flatter resin layer. Furthermore,
570 the HAZ and taper of the manufactured micro-holes were measured to evaluate the
571 machining quality of the two methods.

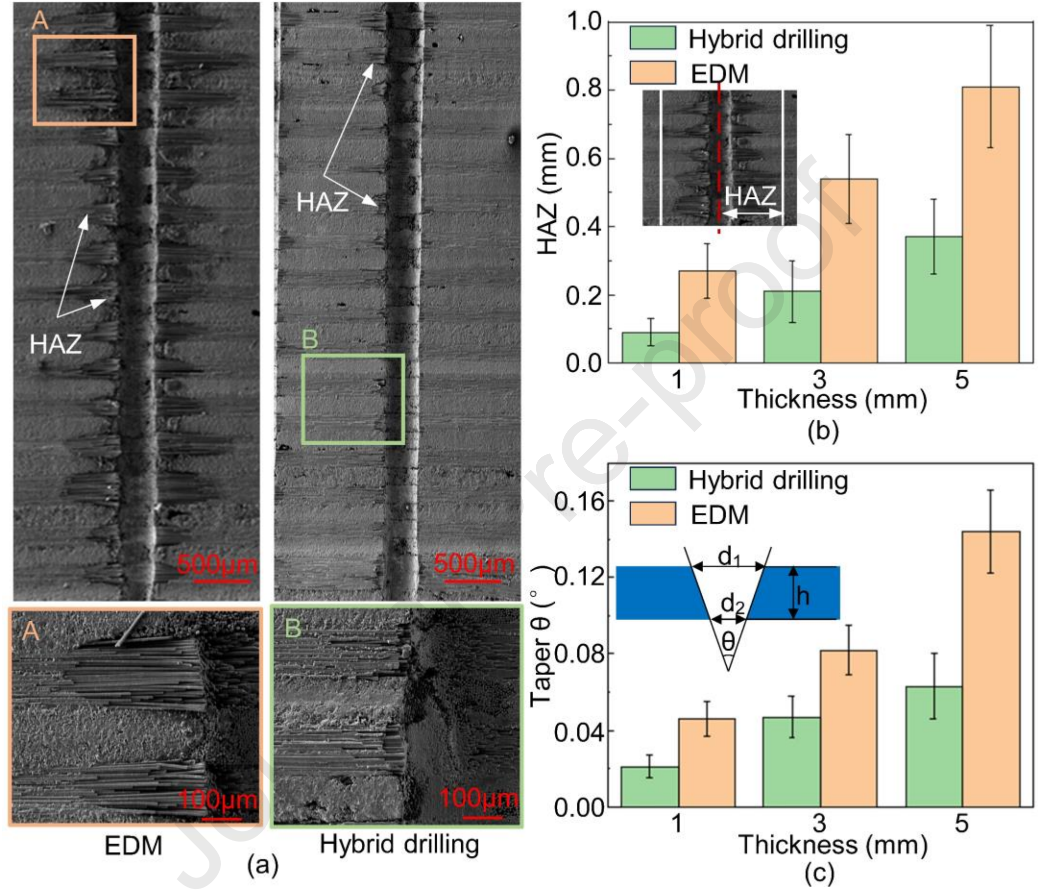


Fig. 20. Effect of different machining methods on machining quality. (a) Profile of machined holes with different machining methods. (b) HAZ of machined holes. (c) Taper of machined holes. The error bars represent the maximum and minimum lengths of the taper for different machining methods.

572 The HAZ was measured directly from the cross-section of the micro-holes. The
573 taper was calculated using Eq. (4).

$$\theta = \tan^{-1}\frac{d_1-d_2}{h} \quad (4)$$

574 where d_1 is the inlet diameter of the machining hole, d_2 is the outlet diameter of the
575 machining hole, and h is and depth of the machining hole.

576 Figs. 20b, c show the statistical results of the HAZ and taper of the micro-holes,
577 respectively. Both the taper and HAZ of the micro-holes manufactured by the hybrid
578 drilling were significantly smaller than those manufactured by EDM, indicating better

579 machining quality. During EDM of CFRP, frequent side discharge and poor discharge
580 stability were the dominant factors that deteriorated machining quality. Fig. 21 shows
581 the schematic and observations of the side discharge. It is evident that the carbon fibre
582 debris produced during the EDM of CFRP holes was significantly larger than ordinary
583 metal debris, which tends to increase the frequency of side discharges between the hole
584 wall and the tool electrode. Additionally, the carbon fibre debris produced by the
585 electrical discharge-mechanical hybrid drilling method was significantly smaller than
586 that produced by EDM (Fig.12). Consequently, side discharges were effectively
587 alleviated during hybrid drilling, resulting in a smaller taper and HAZ.

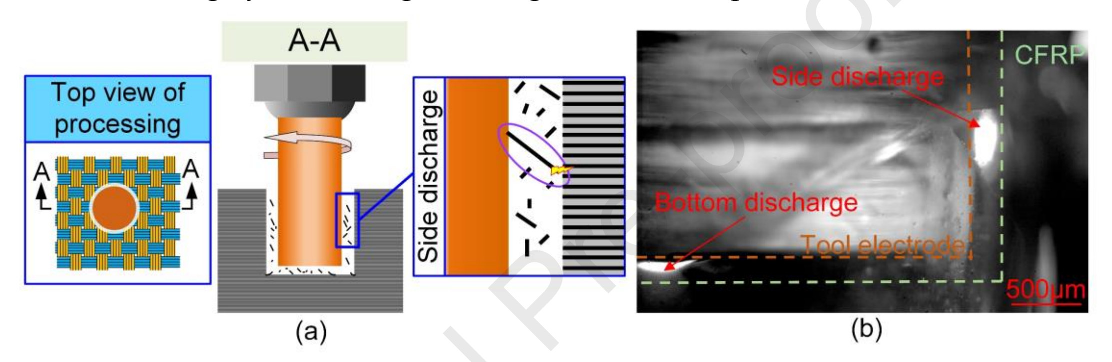


Fig. 21. Principle and observation of side discharge. (a) Schematic of side discharge. (b) Observation diagram of side discharge.

588 The statistical results of the discharge state during the hybrid drilling and EDM of
589 the carbon fibre layer are shown in Fig.19. It is evident that hybrid drilling has a better
590 discharge state than EDM, owing to the small debris produced by hybrid drilling, which
591 are easy to remove from the discharge gap (Fig. 12). A stable discharge state ensures
592 uniform material removal, resulting in a smooth machined surface. It also suppresses
593 severe thermal damage to the machined surface caused by arc discharge, such as
594 exposed carbon fibre and non-flat resin layers.

595 The experimental results presented above demonstrate that the hybrid drilling
596 method for machining CFRP micro-holes achieves simultaneous improvements in both
597 machining efficiency and quality, compared to conventional EDM. Furthermore, a
598 series of experiments were conducted to investigate the effects of process parameters,
599 including peak discharge current and pulse frequency, on the machining efficiency and
600 quality of the hybrid drilling method. The results of these experiments are presented in
601 Appendix 2.

602 **4.2.3 Wear of tool electrodes**

603 Fig. 22 shows the electrode wear when machining holes in the CFRP using different
604 machining methods. The tool electrode wear was slightly less for electrical discharge-
605 mechanical hybrid drilling compared to EDM. With increasing machining depth, the
606 difference in electrode wear between hybrid drilling and EDM did not change
607 significantly.

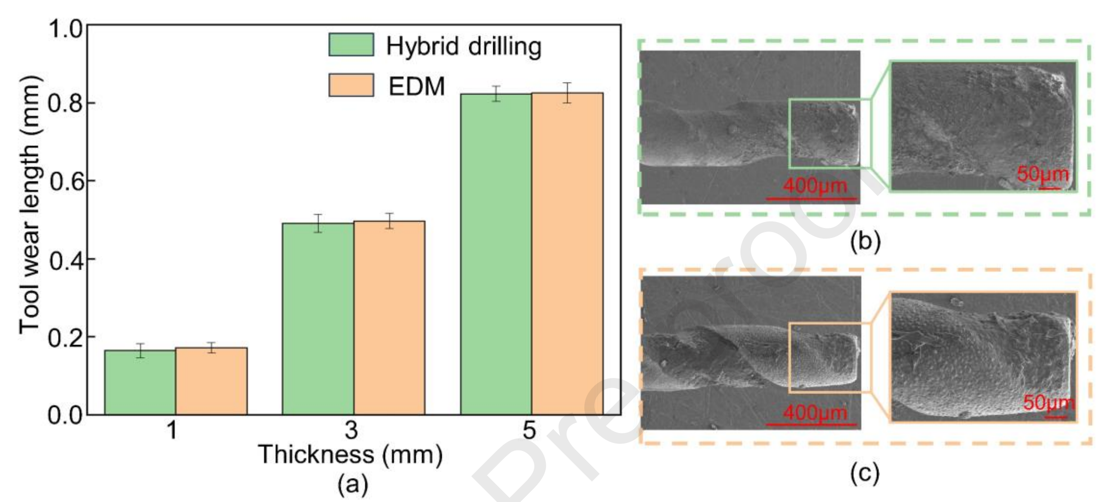


Fig. 22. Effect of different machining methods on the tool electrode wear. (a) Tool electrode wear lengths for machining CFRP of different thicknesses using different machining methods. The error bars represent the maximum and minimum lengths of tool electrode wear for different machining methods. (b) SEM observations of tool electrodes after electrical discharge-mechanical hybrid drilling of the CFRP (thickness: 5 mm). (c) SEM observations of tool electrodes after EDM of the CFRP (thickness: 5 mm).

608 During electrical discharge-mechanical hybrid drilling of CFRP, tool electrode
609 wear consists of two parts: discharge erosion of the tool electrode during EDM of
610 carbon fibre, and wear of the tool electrode during mechanical drilling of the resin. To
611 quantitatively investigate the effect of EDM and mechanical drilling processes on
612 electrode wear during the electrical discharge-mechanical hybrid drilling of the CFRP,
613 EDM of carbon fibre and mechanical drilling of resin were executed separately, and the
614 corresponding electrode wear was measured.

615 A tungsten steel drill was used as the tool electrode to machine carbon fibre using
616 EDM under the same machining parameters as in hybrid drilling, and the electrode wear
617 was evaluated using T_c. Mechanical drilling experiments on the resin were also
618 conducted, and tool wear was evaluated using T_e. The electrode wear T_c and tool wear
619 T_e were calculated using Eqs. (5) and (6), respectively.

$$T_c = \frac{L_{\text{tool}}}{L_c} \tag{5}$$

$$T_e = \frac{L_{\text{tool}}}{L_e} \tag{6}$$

620 where L_{tool} is the electrode/tool wear length after machining, and L_c and L_e are the
621 thicknesses of the carbon fibre and resin layers, respectively.

622 Fig. 23a and c show the tool wear lengths during EDM of carbon fibre and during
623 mechanical drilling of resin, respectively. Using Eq. (5) and Eq. (6), the electrode wear
624 T_c generated by EDM and the electrode wear T_e generated by mechanical drilling were
625 calculated to be 23.9% and 4.3%, respectively. As shown in Fig. 23b and d, the electrode
626 wear was severe during EDM of carbon fibre, and the tool tip was completely removed
627 by the discharge. This was because the material for the finished micro drills was
628 tungsten steel, which is susceptible to discharge removal during EDM. Severe wear of
629 the tool electrode in EDM of carbon fibre was the primary reason why the advantages
630 of hybrid drilling decrease as the machining depth increases.

631 In this study, the aspect ratio of the micro-holes with a diameter of 330μm reached
632 15.1, significantly exceeding previous related research findings (Fig. 1). In fact, the
633 machining depth can continue to increase with longer machining times. However, the
634 machining efficiency gradually decreases with increasing machining depth, due to the
635 accelerated wear of the tool electrode and the poor debris removal conditions. To
636 address this problem, electrical corrosion-resistant materials can be used to fabricate
637 specialized tool electrodes for electrical discharge-mechanical hybrid drilling. However,
638 the application of this hybrid drilling method is obviously limited due to the increased
639 costs caused by customizing the tool electrodes.

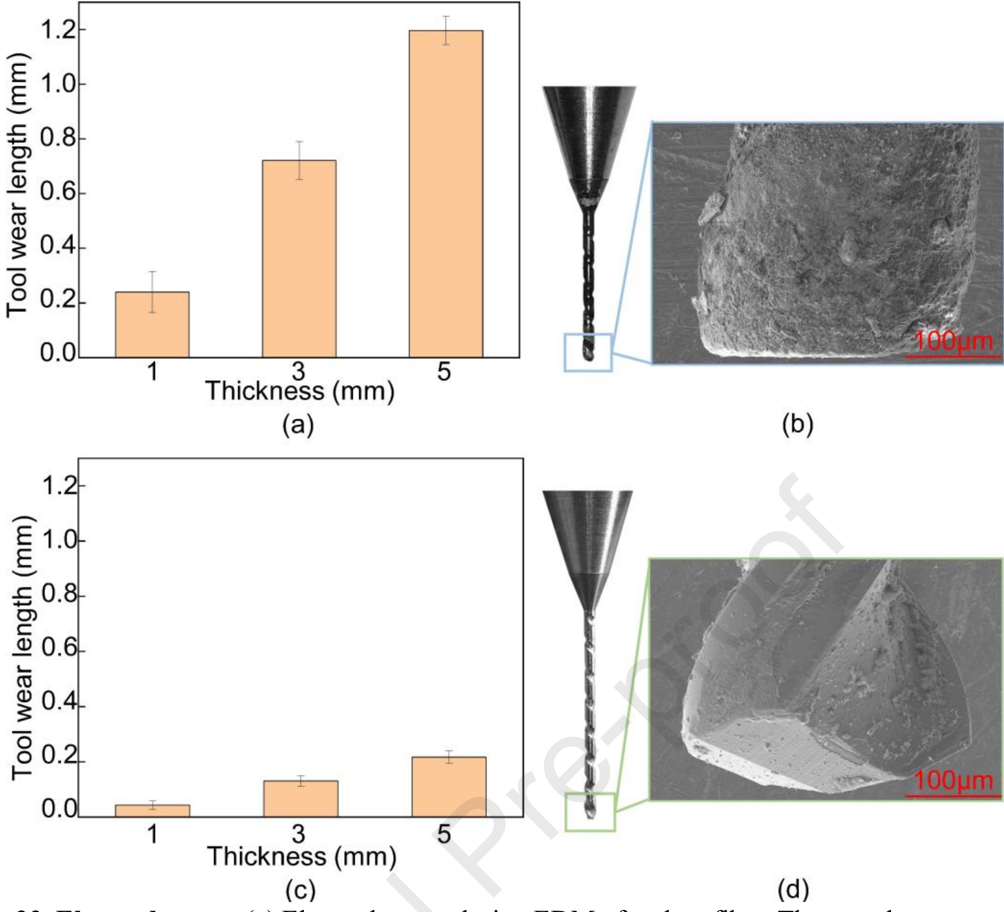


Fig. 23. Electrode wear. (a) Electrode wear during EDM of carbon fibre. The error bars represent the longest and shortest tool electrode wear lengths. (b) Observation of electrode wear when machining carbon fibre (carbon fibre thickness is 5 mm). (c) Electrode wear during drilling of resin. The error bars represent the longest and shortest tool electrode wear lengths. (d) Observation of electrode wear when machining resin (resin thickness is 5 mm).

640 The electrode wear when machining CFRP using electrical discharge-mechanical
641 hybrid drilling can be calculated using Eq. (7).

$$L = T_c \times h_c + T_e \times h_e \quad (7)$$

642 where h_c and h_e are the total thicknesses of the carbon fibre and resin layers in the CFRP,
643 respectively.

644 To demonstrate the effectiveness of Eq. (7), a single layer of CFRP with a carbon
645 fibre layer of 300 μm and a resin layer of 500 μm was machined using electrical
646 discharge-mechanical hybrid drilling, and the electrode wear was measured. Ten
647 repetitive experiments were performed to measure the electrode wear to eliminate the
648 effect of randomness on the machining results. Fig. 24 shows that the maximum
649 deviation of the theoretical wear length from the experimental results is 5.3 μm and the
650 predicted deviation is less than 6%, proving the validity of the theoretical equations (Eq.
651 (7)). This supports the prediction of electrode wear during electrical discharge-

652 mechanical hybrid drilling of CFRP under conditions where the proportion of carbon
653 fibre and resin can be determined.

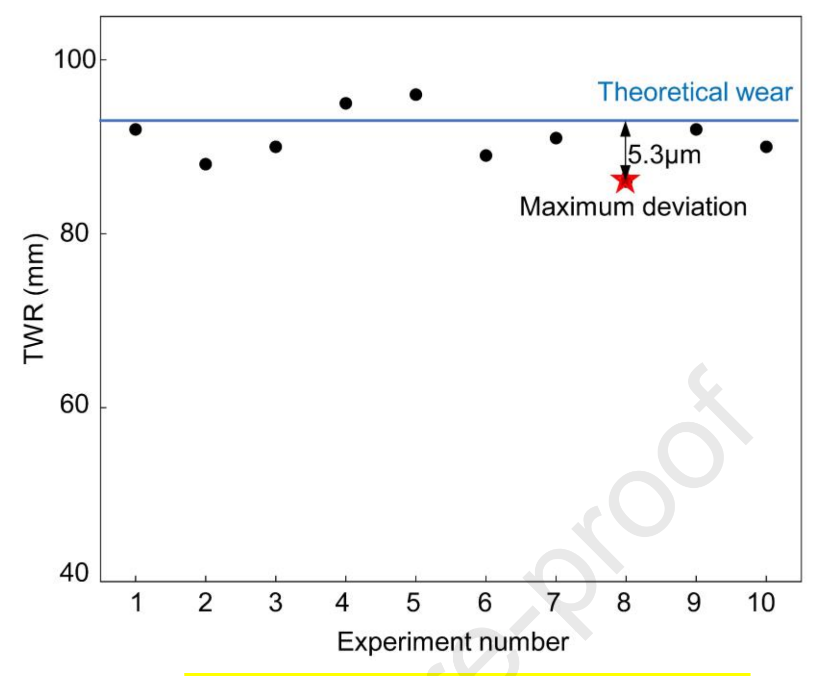


Fig. 24. Electrode wear of electrical discharge-mechanical hybrid drilling.

654 **4.3 Application expansion of non-flat machining**

655 In actual manufacturing processes, the surface of the workpiece is not always
656 perpendicular to the tool electrode. Thus, evaluating the applicability of the electrical
657 discharge-mechanical hybrid drilling method for non-flat structures is essential. Fig. 25
658 shows an analysis of the material removal process during micro-holes machining on the
659 surface of a tilted CFRP workpiece using a hybrid drilling method.

660 As the tool electrode gradually approaches the workpiece, a discharge breakdown
661 occurs with the carbon fibre, which have good electrical conductivity, allowing the
662 carbon fibre to be effectively removed by EDM (Fig. 25b). Meanwhile, the resin
663 adjacent to the carbon fibre is thermally decomposed due to the heat generated during
664 the EDM. Then, as the tool electrode continues to feed downward, both EDM and
665 mechanical drilling are performed simultaneously to remove the carbon fibre and resin,
666 respectively, thereby achieving efficient hybrid drilling. In Figs. 25c and 25d, the red
667 area indicates the portion of carbon fibre removed by EDM; the green area represents
668 the adjacent resin area removed due to the heat generated during EDM of carbon fibre;
669 and the blue area clearly shows the portion of resin removed by mechanical drilling.

670 Since the servo feed control strategy used during hybrid drilling relies on the significant
671 difference in electrical conductivity between carbon fibre and resin, its effectiveness is
672 independent of the distribution of carbon fibre and resin in CFRP along the feed
673 direction. Therefore, the electrical discharge-mechanical hybrid drilling method still
674 offer significant advantages in the micro-hole processing of inclined CFRP components.

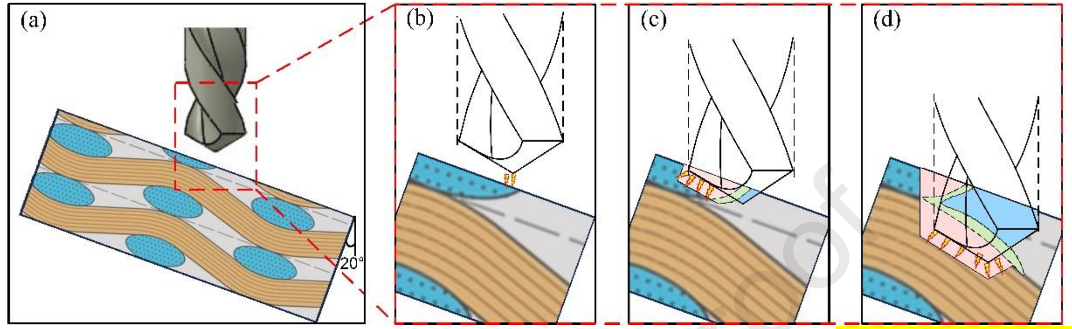


Fig. 25. Schematic diagram of non-flat CFRP machining process using electrical discharge-mechanical hybrid drilling method. (a) Schematic diagram of machining position. (b) The case of removal only by electrical discharge. (c) (d) The case of removal by electrical discharge, heat and mechanical drilling.

675 Furthermore, electrical discharge-mechanical hybrid drilling was employed to
676 process micro-holes in CFRP sheets at inclination angles of 20°, 40°, and 60°. The
677 processing parameters remain consistent for all CFRP workpieces, as shown in Table 2.
678 Fig. 26 shows the cross-sectional morphology of the machined hole as observed by
679 SEM. Observations reveal that the surface morphology of CFRP micro-holes at
680 different inclined angles shows no significant differences, and the exposed carbon fibre
681 area is consistently very small. The protrusions in Fig. 26 is a built-up edge generated
682 during the sample preparation for observation of the machined hole profile and is not
683 related to the hole manufacturing process. To further characterise the influence of the
684 inclination angle on the machining quality, the HAZ of the machined holes was
685 measured, and the measurement results are shown in Fig. 27. The variations of the
686 inclination angle of the machined hole does not affect the machining quality, which
687 further confirms that the hybrid drilling method is also applicable to the machining of
688 CFRP inclined holes.

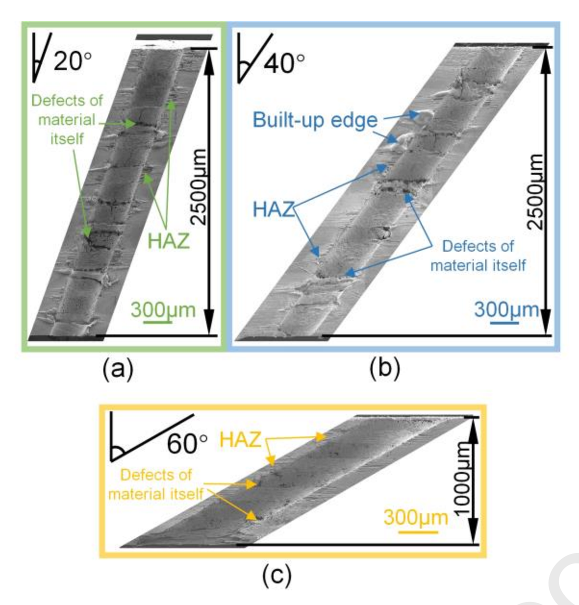


Fig. 26. Non-flat processing results of hybrid drilling. (a) 20° inclined surface processing result. (b) 40° inclined surface processing result (c) 60° inclined surface processing result.

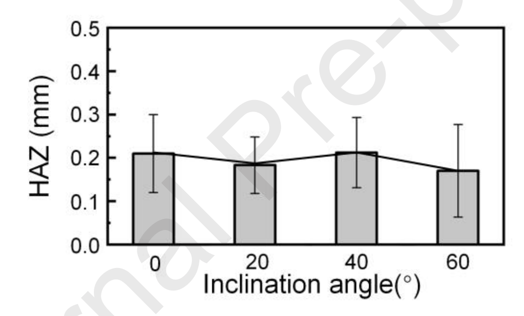


Fig. 27. The difference of HAZ of CFRP micro-holes processed by hybrid drilling at different inclination angles. The error bar is the maximum and minimum size of multiple HAZ defects.

689 ## 5 Conclusion

690 In this study, an electrical discharge-mechanical hybrid drilling method was
691 proposed to achieve deep micro-hole machining of CFRP. During this hybrid drilling
692 process, EDM and mechanical drilling are performed alternately or simultaneously to
693 remove the carbon fibre and resin layers, which integrates the advantages of both EDM
694 and mechanical drilling. The developed electrical discharge-mechanical hybrid drilling
695 method provides a new solution for high-quality micromachining of advanced
696 composites with similar material systems. The main conclusions of this study are
697 summarised as follows.

698 (1) During electrical discharge-mechanical hybrid drilling of CFRP, EDM and
699 mechanical drilling can be accurately and automatically switched to process the carbon

700 fibre and resin layers separately using the servo-control strategy based on monitored
701 gap voltage waveform, attributed to the significant electrical conductivity difference
702 between carbon fibre and resin layer. The knowledge gained from the servo control
703 strategy during electrical discharge-mechanical hybrid drilling contributes to the
704 realization of hybridization of other machining methods for high quality and efficient
705 machining of multilayer composites.

706 (2) High-quality and high-efficiency machining of CFRP deep micro-holes, with
707 a diameter of 332 μm and the machining depth of 5000 μm, was realized for the first
708 time using the proposed electrical discharge-mechanical hybrid drilling method. This
709 proves the feasibility and unique advantages of the hybrid drilling method for
710 micromachining of multilayer composites with large variations in internal properties.

711 (3) The electrical discharge-mechanical hybrid drilling exhibits significantly
712 higher machining efficiency than the EDM, owing to the combined effect of the high
713 efficiency of mechanical drilling for the resin layer and the better discharge state during
714 EDM of carbon fibre layer. When machining deep micro-holes in CFRP, the machining
715 efficiency of hybrid drilling is 29.1% higher than that of EDM.

716 (4) The size of the carbon fibre debris produced by hybrid drilling of CFRP is
717 significantly smaller than that produced by EDM. This phenomenon can be attributed
718 to the unique conical geometry of the tool electrode in hybrid drilling facilitates the
719 optimisation of the discharge position, ensuring that the discharge is mainly
720 concentrated at the exposed ends of the carbon fibre in the machined area. This
721 effectively avoids the large carbon fibre debris generated by the spalling of carbon fibre
722 between two discharge points on a single carbon fibre. The smaller size of the debris
723 during machining contributes to a reduction in the frequency of side discharge, resulting
724 in improved machining stability and quality.

725 (5) The hole taper and HAZ are important indicators of the quality of CFRP deep
726 micro-hole machining. The hole taper and HAZ of CFRP deep micro-holes machined
727 by electrical discharge-mechanical hybrid drilling are significantly reduced by 56.25%
728 and 54.32% in comparison to EDM respectively, providing better machining accuracy

729 and surface integrity.

730 Further research will focus on the fabrication of special tool electrodes for
731 electrical discharge-mechanical hybrid drilling using electrically corrosion-resistant
732 materials with the aim of enhancing the effectiveness of this method in machining
733 CFRP micro-holes.

734 **Appendix 1**

735 The electrical discharge-mechanical hybrid drilling method is not only effective in
736 the machining of CFRP, but also can be extended to the machining of deep micro-hole
737 in similar composites. It is particularly suitable for laminated composites, where the
738 reinforcing phase is electrically conductive and can be accurately removed by EDM,
739 while the matrix phase is non-conductive and low-hardness, which can be easily peeled
740 off by mechanical drilling. To empirically demonstrate its wide applicability, carbon
741 fibre reinforced polyamide (CF/PA) and carbon fibre reinforced polyether ether ketone
742 (CF/PEEK) were specially selected as experimental objects for the machining tests. Fig.
743 A1 shows the morphology of the machined holes, and the heat affected zone (HAZ) of
744 the machined holes is larger than that of CFRP owing to the low thermal decomposition
745 temperature of the matrix phases PA and PEEK. The results indicate that effective
746 machining can be achieved using this hybrid drilling method, thus fully verifying its
747 general applicability in the machining of similar materials.

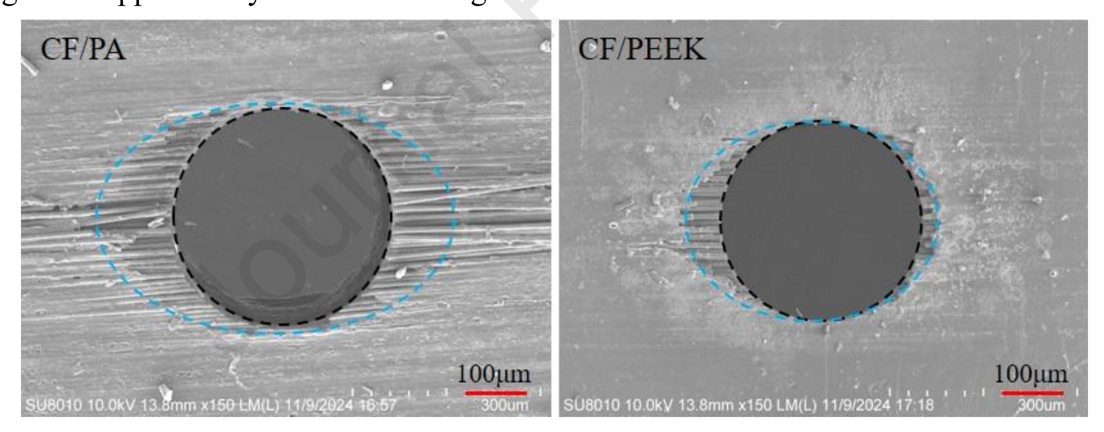


Fig. A1. Machining results for similar kinds of composite material

748 **Appendix 2**

749 This study analyzed the effects of peak discharge current and pulse frequency on
750 machining efficiency and quality under the machining conditions detailed in Table 2
751 (Section 3.2.1). Fig. A2(a) shows the variation in machining efficiency with respect to
752 the peak discharge current. It is observed that higher peak discharge currents result in
753 higher material removal rates (MRR). This is because higher peak discharge current
754 means larger discharge energy is used for machining. In contrast, machining efficiency

755 remains largely unaffected by an increase in pulse frequency in this study (Fig. A2 (b)).
756 Considering the 50% duty cycle of the pulse power supply, an increase in pulse
757 frequency leads to a proportional decrease in the discharge duration within each pulse
758 cycle, thereby reducing the energy per discharge in the same proportion. However, it
759 also results in a proportional increase in the number of discharges per unit time.
760 Consequently, the total discharge energy per unit of time remains constant, indicating
761 that machining efficiency is significantly unaffected by changes in pulse frequency.

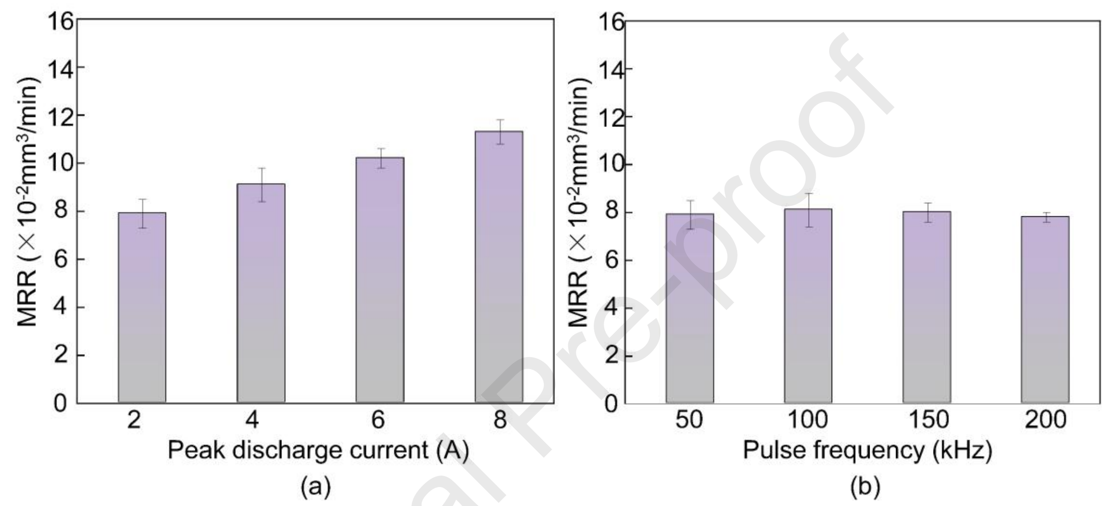


Fig. A2. Influence of key electrical parameters on machining efficiency. The error bars represent the highest and lowest data of the MRR. (a) Influence of peak discharge current on MRR (pulse frequency: 50kHz). (b) Influence of pulse frequency on MRR (peak discharge current: 2A).

762 Fig. A3(a) and Fig. A3(b) show the influences of peak discharge current and the
763 pulse frequency on the heat-affected zone (HAZ), respectively. It is evident from Fig.
764 A3(a) that the HAZ shows an expansion trend as the peak discharge current increases.
765 As discussed in sections 4.2.2, in EDM of CFRP, the HAZ are mainly affected by the
766 side discharge between the hole side surface and the tool electrode, which occurs during
767 debris removal. An increase in peak discharge current leads to an increase in discharge
768 energy per pulse, causing deeper resin removal on the hole side surface and exposing
769 more carbon fiber, thereby expanding the HAZ. Furthermore, Fig. A3(b) indicates that
770 an increase in pulse frequency reduces the HAZ. This is because an increase in pulse
771 frequency shortens the discharge duration on the hole side surface, which contributes
772 to the inhibition of HAZ formation.

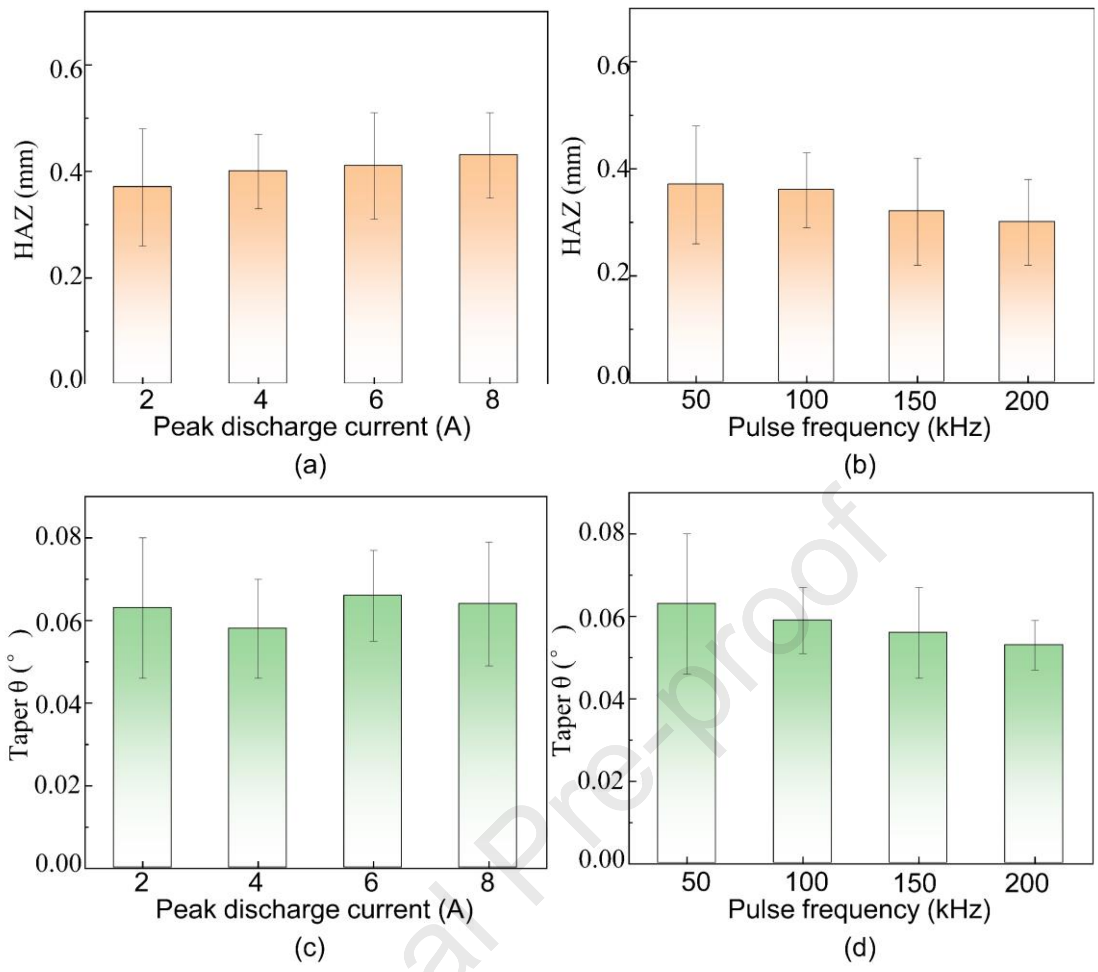


Fig. A3. Influence of key electrical parameters on machining quality. The error bars represent the highest and lowest data. (a) Influence of peak discharge current on HAZ (pulse frequency: 50kHz). (b) Influence of pulse frequency on HAZ (peak discharge current: 2A). (c) Influence of peak current on machining taper (pulse frequency: 50kHz). (d) Influence of pulse frequency on machining taper (peak discharge current: 2A).

773 Fig. A3(c) shows the effect of peak discharge current on hole taper. Although an
774 increase in peak discharge current tends to increase the hole taper due to increased
775 discharge energy on the hole side surface, higher discharge energy reduces the time
776 needed for hole machining. Shorter machining times result in a reduced side discharge
777 time, which contributes to suppressing the taper of the machined hole. Therefore, the
778 peak discharge current has little effect on the hole taper. In contrast, the taper of the
779 machined hole exhibits a decreasing trend with increasing pulse frequency (Fig. A3 (d)).
780 This is owing to the fact that an increase in pulse frequency reduces the discharge
781 energy per pulse, thereby facilitating the reduction of hole taper.

782 **Reference**

783 [1] Y. Liu, W. Zhuang, S. Wu. Damage to carbon fibre reinforced polymers (CFRP) in hole-
784 clinched joints with aluminium alloy and CFRP, Composite Structures 234 (2020),
785 http://doi.org/10.1016/j.compstruct.2019.111710.
786 [2] M. Hamed, C. Zhang, A. Khan, M. Saleem, M. Musanur. Holistic review of drilling on CFRP
787 composites: Techniques, FEM, sustainability, challenges, and advances, The International
788 Journal of Advanced Manufacturing Technology 21 (2024), https://doi.org/10.1007/s00170-
789 024-14317-w.
790 [3] P. Alam, D. Mamalis, C. Robert, C. Floreani, C. Ó Brádaigh. The fatigue of carbon fibre
791 reinforced plastics - A review, Composites Part B 166 (2019),
792 https://doi.org/10.1016/j.compositesb.2019.02.016.
793 [4] E. Hui, R. Howe, M. Rodgers. Single-step assembly of complex 3-D microstructures, IEEE
794 (2000), http://doi.org/10.1109/MEMSYS.2000.838586.
795 [5] M. Ramakrishnan, G. Rajan, Y. Semenova, G. Farrell. Overview of fiber optic sensor
796 technologies for strain/temperature sensing applications in composite materials, Sensors 16
797 (2016), http://doi.org/10.3390/s16010099.
798 [6] T. Das, P. Ghosh, N. Das. Preparation, development, outcomes, and application versatility of
799 carbon fiber-based polymer composites: a review, Advanced Composites and Hybrid Materials
800 2 (2019), http://doi.org/10.1007/s42114-018-0072-z.
801 [7] Z. Jia, R. Fu, B. Niu, B. Qian, Y. Bai, F. Wang. Novel drill structure for damage reduction in
802 drilling CFRP composites, International Journal of Machine Tools & Manufacture 110 (2016),
803 http://dx.doi.org/10.1016/j.ijmachtools.2016.08.006.
804 [8] X. Wang, P. Kwon, C. Sturtevant, D. Kim, J. Lantrip. Tool wear of coated drills in drilling
805 CFRP, Journal of Manufacturing Processes 15 (2013),
806 http://dx.doi.org/10.1016/j.jmapro.2012.09.019.
807 [9] J. Xu, N. Geier, J. Shen, V. Krishnaraj, S. Samsudeensadham. A review on CFRP drilling:
808 fundamental mechanisms, damage issues, and approaches toward high-quality drilling, Journal
809 of Materials Research and Technology 24 (2023), http://doi.org/10.1016/j.jmrt.2023.05.023.
810 [10] D. Wang, P. Onawumi, S. Ismail, H. Dhakal, I. Popov, V. Silberschmidt, A. Roy. Machinability
811 of natural-fibre-reinforced polymer composites: Conventional vs ultrasonically-assisted
812 machining, Composites Part A-Applied Science and Manufacturing 119 (2019),
813 http://doi.org/10.1016/j.compositesa.2019.01.028.
814 [11] M. Li, M. Huang, X. Yang, S. Li, K. Wei. Experimental study on hole quality and its impact on
815 tensile behavior following pure and abrasive waterjet cutting of plain woven CFRP laminates,
816 The International Journal of Advanced Manufacturing Technology 99 (2018),
817 http://doi.org/10.1007/s00170-018-2589-2.
818 [12] X. Liu, L. Li, S. Yang, M. Xu, B. Wang, Y. Jiang. Optimization of nanosecond laser drilling
819 strategy on CFRP hole quality, Journal of Materials Processing Technology 332 (2024),
820 https://doi.org/10.1016/j.jmatprotec.2024.118559.
821 [13] J. Nyaboro, M. Ahmed, H. El-Hofy, M. El-Hofy. Fluid-structure interaction modeling of the
822 abrasive waterjet drilling of carbon fiber reinforced polymers, Journal of manufacturing
823 processes 58 (2020), http://doi.org/10.1016/j.jmapro.2020.08.035.
824 [14] J. Schwartzentruber, M. Papini, J. Spelt. Characterizing and modelling delamination of carbon-
825 fiber epoxy laminates during abrasive waterjet cutting, Composite. A Apply Science and

826 Manufacture. 112 (2018), http://doi.org/10.1016/j.compositesa.2018.06.014.
827 [15] P. Wang, Z. Zhang, B. Hao, D. Liu, Y. Zhang, T. Xue, G. Zhang. Reducing the taper and the
828 heat-affected zone of CFRP plate by Micro fluid assisted laser induced plasma micro-drilling,
829 Journal of Manufacturing Processes 103 (2023), http://doi.org/10.1016/j.jmapro.2023.08.043.
830 [16] W. Li, G. Zhang, Y. Huang, Y. Rong. Drilling of CFRP plates with adjustable pulse duration
831 fiber laser, Materials and Manufacturing Processes 36 (2021),
832 https://doi.org/10.1080/10426914.2021.1905838.
833 [17] Y. Liu, L. Wang, Y. Guo, Y. Feng, Y. Du. Investigation on surface morphology and phase
834 transition characteristics in EDM for 8YSZ TBC on Inconel 718 superalloy, The International
835 Journal of Advanced Manufacturing Technology 124 (2023), https://doi.org/10.1007/s00170-
836 022-10738-7.
837 [18] S. Gong, Z. Wang, X. He, Y. Wang. Material removal mechanisms, processing characteristics
838 and surface analysis of Cf-ZrB2-SiC in micro-EDM, Ceramics International 48 (2022),
839 https://doi.org/10.1016/j.ceramint.2022.06.289.
840 [19] W. Lau, M. Wang, W. Lee, Electrical-discharge machining of carbon-fiber composite-materials,
841 International Journal of Machine Tools and Manufacture, 30 (1990),
842 http://doi.org/10.1016/0890-6955(90)90138-9.
843 [20] S. Habib, A. Okada. Influence of electrical discharge machining parameters on cutting
844 parameters of carbon fiber reinforced plastic, Machining Science and Technology 20 (2016),
845 http://doi.org/10.1080/10910344.2015.1133914.
846 [21] J. Sheikh-Ahmad. Hole quality and damage in drilling carbon/epoxy composites by electrical
847 discharge machining, Materials and Manufacturing Processes 31 (2016),
848 http://doi.org/10.1080/10426914.2015.1048368.
849 [22] R. Kumar, P. Agrawal, I. Singh. Fabrication of micro holes in CFRP laminates using EDM,
850 Journal of Manufacturing Processes 31 (2018), https://doi.org/10.1016/j.jmapro.2018.01.011.
851 [23] P. Koshy, V. Jain, G. Lal. Grinding of cemented carbide with electrical spark assistance, The
852 Journal of Materials Processing Technology 72 (1997), https://doi.org/10.1016/S0924-
853 0136(97)00130-1.
854 [24] I. Menzies, P. Koshy. Assessment of abrasion-assisted material removal in wire EDM, CIRP
855 Annals-Manufacturing Technology 57 (2008), https://doi.org/10.1016/j.cirp.2008.03.135.
856 [25] X. Rao, F. Zhang, Y. Lu, X. Luo, F. Chen. Surface and subsurface damage of reaction-bonded
857 silicon carbide induced by electrical discharge diamond grinding, International Journal of
858 Machine Tools and Manufacture 154 (2020),
859 https://doi.org/10.1016/j.ijmachtools.2020.103564.
860 [26] A. Hsue, Y. Chang. Toward synchronous hybrid micro-EDM grinding of micro-holes using
861 helical taper tools formed by Ni-Co/diamond Co-deposition, Journal of Materials Processing
862 Technology 234 (2016), https://doi.org/10.1016/j.jmatprotec.2016.04.009.
863 [27] N. Ramanujam, S. Dhanabalan, D. Kumar, N. Jeyaprakash. Investigation of Micro-Hole
864 Quality in Drilled CFRP Laminates Through CO2 Laser, Arabian Journal for Science and
865 Engineering 46 (2021), https://doi.org/10.1007/s13369-021-05505-x.
866 [28] X. Liu, L. Li, S. Yang, M. Xu, M. Zhong, B. Wang, Y. Jiang. Optimization of nanosecond laser
867 drilling strategy on CFRP hole quality, Journal of Materials Processing Technology 332 (2024),
868 https://doi.org/10.1016/j.jmatprotec.2024.118559.
869 [29] X. Liu, S. Yang, Y. Gao, M. Xu, Y. Wan, M. Wu, L. Li, C. Wang, M. Zhong, B. Wang, Y. Jiang.

870 Hole quality and thermal defects in drilled CFRP by nanosecond pulsed laser, The International
871 Journal of Advanced Manufacturing Technology 132 (2024), https://doi.org/10.1007/s00170-
872 024-13562-3.
873 [30] P. Wang, Z. Zhang, D. Liu, W. Qiu, Y. Zhang, G. Zhang. Comparative investigations on
874 machinability and surface integrity of CFRP plate by picosecond laser vs laser induced plasma
875 micro-drilling, Optics & Laser Technology 151 (2022),
876 https://doi.org/10.1016/j.optlastec.2022.108022.
877 [31] H. Jiang, C. Ma, M. Li, Z. Cao. Femtosecond Laser Drilling of Cylindrical Holes for Carbon
878 Fiber-Reinforced Polymer (CFRP) Composites, Molecules 10 (2021),
879 https://doi.org/10.3390/molecules26102953.
880 [32] U. Teicher, S. Müller, J. Münzner, A. Nestler. Micro-EDM of carbon fiber reinforced plastics,
881 The Seventeenth CIRP Conference on Electro Physical and Chemical Machining (ISEM) 6
882 (2013), https://doi.org/10.1016/j.procir.2013.03.092.
883 [33] S. Park, G. Kim, W. Lee, B. Min, S. Lee, T. Kim. Micro-hole Machining on Precision CFRP
884 Components Using Electrical Discharge Machining, International Conference on Composite
885 Materials, 18 (2015), https://www.researchgate.net/publication/281719904.
886 [34] A. Korlos, D. Tzetzis, G. Mansour. Investigation of the electro-discharge open-hole machining
887 on the structural behavior of carbon fiber reinforced polymers, Applied Mechanics and
888 Materials 657 (2014), https://doi.org/10.4028/www.scientific.net/AMM.657.321.
889 [35] A. Ito, S. Hayakawa, F. Itoigawa, T. Nakamura. Effect of Short-Circuiting in Electrical
890 Discharge Machining of Carbon Fiber Reinforced Plastics, Journal of Advanced Mechanical
891 Design, Systems, and Manufacturing 6 (2012), https://doi.org/10.1299/jamdsm.6.808.
892 [36] M. Karataş, A. Motorcu, H. Gökkaya. Study on delamination factor and surface roughness in
893 abrasive water jet drilling of carbon fiber-reinforced polymer composites with different fiber
894 orientation angles, Journal of the Brazilian Society of Mechanical Sciences and Engineering
895 22 (2021), https://doi.org/10.1007/s40430-020-02741-4.
896 [37] M. Li, M. Huang, X. Yang, S. Li, K. Wei. Experimental study on hole quality and its impact on
897 tensile behavior following pure and abrasive waterjet cutting of plain woven CFRP laminates,
898 The International Journal of Advanced Manufacturing Technology 99 (2018),
899 https://doi.org/10.1007/s00170-018-2589-2.
900 [38] I. Popan, V. Bocănet, S. Softic, A. Popan, N. Panc, N. Balc. Artificial Intelligence Model Used
901 for Optimizing Abrasive Water Jet Machining Parameters to Minimize Delamination in Carbon
902 Fiber-Reinforced Polymer, Applied Sciences 14 (2024), https://doi.org/10.3390/app14188512.
903 [39] M. Karataş, A. Motorcu, H. Gökkaya. Optimization of machining parameters for kerf angle
904 and roundness error in abrasive water jet drilling of CFRP composites with different fiber
905 orientation angles, Journal of the Brazilian Society of Mechanical Sciences and Engineering
906 42 (2022), https://doi.org/10.1007/s40430-020-2261-2.
907 [40] D. Geng, Y. Teng, Y. Liu, Z. Shao, X. Jiang, D. Zhang. Experimental study on drilling load and
908 hole quality during rotary ultrasonic helical machining of small-diameter CFRP holes, Journal
909 of Materials Processing Technology 270 (2019),
910 https://doi.org/10.1016/j.jmatprotec.2019.03.001.
911 [41] K. John, S. Kumaran. A feasible strategy to produce quality holes using temperature-assisted
912 drilling on CFRP, The International Journal of Advanced Manufacturing Technology 110
913 (2020), https://doi.org/10.1007/s00170-020-06089-w.

914 [42] M. Li, G. Gan, B. Li, X. Yang. Whole-field strain analysis and strength prediction of fiber laser
915 machined CFRP laminate at elevated temperature, Polymer Composites 41 (2020),
916 https://doi.org/10.1002/pc.25565.
917 [43] M. Batista, I. Basso, F. Toti, A. Rodrigues, J. Tarpani. Cryogenic drilling of carbon fibre
918 reinforced thermoplastic and thermoset polymers, Composite Structures 251 (2020),
919 https://doi.org/10.1016/j.compstruct.2020.112625.
920 [44] J. Xu, C. Li, S. Mi, Q. An, M. Chen. Study of drilling-induced defects for CFRP composites
921 using new criteria, Composite Structures 201 (2018),
922 https://doi.org/10.1016/j.compstruct.2018.06.051.
923 [45] B. Zhang, F. Wang, X. Wang, Y. Li, Q. Wang. Optimized selection of process parameters based
924 on reasonable control of axial force and hole-exit temperature in drilling of CFRP, The
925 International Journal of Advanced Manufacturing Technology 110 (2020),
926 https://doi.org/10.1007/s00170-020-05868-9.
927 [46] G. Poulachon, J. Outeiro, C. Ramirez, V. André, G. Abrivard. Hole surface topography and tool
928 wear in CFRP drilling, 3rd CIRP Conference on Surface Integrity 45 (2016),
929 http://creativecommons.org/licenses/by-nc-nd/4.0/.
930 [47] T. Ohkubo, M. Tsukamoto, Y. Sato. Numerical simulation of combustion effects during laser
931 processing of carbon fiber reinforced plastics, Appl Physics A-Materials Science and
932 Processing 122 (2016), https://doi.org/10.1007/s00339-016-9735-1.
933 [48] R. Negarestani, M. Sundar, M. Sheikh, P. Mativenga, L. Li, Z. Li, P. Chu, C. Khin, H. Zheng,
934 G. Lim. Numerical simulation of laser machining of carbon-fibre-reinforced composites,
935 Proceedings of the Institution of Mechanical Engineers, Part B: Journal of Engineering
936 Manufacture 224 (2010), https://doi.org/10.1243/09544054jem1662.
937 [49] J. Tao, J. Ni, A. Shih. Modeling of the anode crater formation in electrical discharge machining,
938 Journal of Manufacturing Science and Engineering 134 (2012),
939 https://doi.org/10.115/1.4005303.
940 [50] H. Xia, M. Kunieda, N. Nishiwaki, Removal amount difference between anode and cathode in
941 EDM process, International Journal of Electrical Machining 1 (1996),
942 https://doi.org/10.2516/ijem.1.45.
943 [51] X. Yue, X. Yang, J. Tian, Z. He, Y. Fan. Thermal, mechanical and chemical material removal
944 mechanism of carbon fiber reinforced polymers in electrical discharge machining, International
945 Journal of Machine Tools & Manufacture 133 (2018),
946 http://doi.org/10.1016/j.ijmachtools.2018.05.004.

Acknowledgement

This work was supported by the National Natural Science Foundation of China (General Program, No. 52375419); and the Postdoctoral Fellowship Program of CPSF (General Program, No. GZC20233455) for providing financial support for this research. The authors gratefully thank Prof. Dragos Axinte and Prof. Zhirong Liao of the University of Nottingham for their suggestions on the experimental plan for this paper.

Highlights

An electrical discharge–mechanical hybrid drilling method is proposed for the first time to machine high-quality micro-holes in CFRP.

The material removal mechanisms of CFRP during hybrid drilling are elucidated with supporting evidence.

High-quality and efficient machining of deep micro-holes in CFRP is achieved, proving the advancement of the developed hybrid drilling method.

The electrical discharge–mechanical hybrid drilling method demonstrates applicability to material systems analogous to CFRP.

Declaration of interests

☒ The authors declare that they have no known competing financial interests or personal relationships that could have appeared to influence the work reported in this paper.

☐ The authors declare the following financial interests/personal relationships which may be considered as potential competing interests: